Analysis of Outage Probability of WLAN & Evaluating Geometry and Coverage of Energy Efficient Light Sources

Rayapati Sushma

A Thesis Submitted to

Indian Institute of Technology Hyderabad

In Fulfillment of the Requirements for

The Degree of Master of Technology

भारतीय प्रौद्योगिकी संस्थान हैदराबाद

Indian Institute of Technology Hyderabad

Department of Electrical Engineering

June 2016

Approval Sheet

This Thesis entitled Analysis of Outage Probability of WLAN & Evaluating Geometry and Coverage of Energy Efficient Light Sources by Rayapati Sushma is approved for the degree of Master of Technology from IIT Hyderabad

Vandana Sharma

(Dr. Vandana Sharma) Examiner
Dept. of Physics
IITH

(Dr. Abhinav Kumar) Examiner
Dept. of Electrical Eng
IITH

G.V.V. Sharma

(Dr G.V.V. Sharma) Adviser
Dept. of Electrical Eng
IITH

Declaration

I declare that this written submission represents my ideas in my own words, and where ideas or words of others have been included, I have adequately cited and referenced the original sources. I also declare that I have adhered to all principles of academic honesty and integrity and have not misrepresented or fabricated or falsified any idea/data/fact/source in my submission. I understand that any violation of the above will be a cause for disciplinary action by the Institute and can also evoke penal action from the sources that have thus not been properly cited, or from whom proper permission has not been taken when needed.

R. Sushma

(Signature)

Rayapati Sushma

(Rayapati Sushma)

EE14MTECH11009

(Roll No.)

Acknowledgements

I would like to thank Dr. G.V.V. Sharma, Dr. Abhinav Kumar and Dr.Vandana Sharma for their constant help and support during this thesis work. They always gave me valuable comments during this work.

I would like to thank my parents and my brother who have been always there for me. Without them, this work had not been possible.

Finally, I would like to thank all my friends in IIT Hyderabad who supported me morally during this period.

Dedication

I dedicate this thesis to my family without them I wouldn't be here.

Abstract

In this thesis, the performance of energy efficient light sources in free space is analyzed. Metrics for irradiance based coverage of a light source are proposed and evaluated analytically. These light sources are generated by arranging point sources in various geometries. The coverage metrics of these sources are calculated over a circular region. Numerical results are then obtained to determine the efficiency of these sources, highlighting the usefulness of this work.

In this thesis, we derive the closed form expressions for the outage probability of a directional and omnidirectional antenna system in the physical layer perspective of Wireless local area networks (WLAN) in lossy wireless networks.Analytical expression for outage probability of directional antenna systems was calculated in the presence of shadowing and Nakagami-m fading considering various pathloss exponent values(i.e., α=2,4). The numerical results shows that our approximate analytical model matches with the simulation results. In this thesis, a directional antenna based wireless local area network (WLAN) is considered in a lossy environment. For the directional WLAN, explicit expressions for outage probability are derived in the presence of shadowing and Rayleigh fading. Further, numerical results are presented that show that the derived results match closely with cross-layer simulation results. The presented results are highly relevant for any cross-layer performance evaluation of directional WLAN based systems.

Contents

Chapter 1

Geometry and Coverage of Energy efficient Light Sources

1.1 Introduction

Light is a electromagnetic wave that propagates through free space. Traditionally, it has been used for making objects visible to the naked eye. Lately, there has been tremendous interest in using it for free space communication [29]. This has simultaneously been accompanied by significant interest in light emitting diodes (LEDs) that have been replacing conventional light sources in almost all applications[13]. Fair amount of existing literature has focused on achieving uniform illuminanace over a planar surface [14]-[19], beginning with the problem of finding the optimal LED geometry at the light source to achieve uniform irradiance [20]. This was done by using the irradiance distributions at the closest points on the incident surface. The case of LEDs using a freeform lens with a large view angle has been considered in [21]. More literature on similar themes is available in [22]-[24].

In all the above, the focus was on achieving uniform irradiance on the incident surface. While this is important in many applications like biomedical instruments, there are other applications e.g. street lights where coverage with a predefined intensity threshold is more important than uniformity. Further, the effect of the distance between the light source and incident area was not thoroughly investigated, though it is an important factor [30]. Also, power consumption of the source, which is a significant parameter, has not been considered in the available literature on uniform irradiance.

In this thesis, we focus on finding appropriate geometry of point light sources for maximizing the coverage over a circular area, assuming that the irradiance in this area is sufficient enough. This is done by also taking the power consumption of the sources into account. In the process, coverage metrics are proposed and analytically evaluated for different geometries. While earlier literature considered LEDs as imperfect Lambertian soures, for simplicity of analysis, point sources are considered in the present work.

1.1.1 Point Sources Vs LEDs

LEDs (Light Emitting Diodes), semiconductor light sources, have been introduced and developed for several decades. LEDs are applied in many devices as indicators and general illumination products such as lighting components. As a green light source, LEDs can provide a long life time and high efficiency light for many applications. However, for some special applications, standard LEDs are not always the perfect choice. Point Source Emitters (PSEs) offer a great alternative in applications needing a precise beam of light such as encoders, machine vision and medical fiber.

A PSE is a semiconductor diode similar in structure to a standard LED, however, the light is emitted through a well-defined circular area, typically 25 μm - 200 μm in diameter. The light produced appears as a spot. The output light produces very narrow, almost parallel viewing angles. These two characteristics are well suited for applications that require a near parallel light source and lower power, as compared with laser diodes.

The first difference in these two structures is emitting light direction. Standard LED output light is directed to the side. In order to refocus the light direction, standard LEDs normally need a reflective cavity to force the light from the side to the top. This can cause light output loss, power dissipation, and variations in final output light beam and viewing angle. However, PSEs emit light to the upper surface through an aperture / window on top of the structure.

The second difference in these two structures is the position of the cathode contact. The cathode contact pad of a standard LED is typically located in the center of the structure, which can obstruct light output due to the top wire bond. SEs can easily solve this problem by locating the cathode contact wire bond to the side of the aperture window, eliminating any obstructions and dark spots.

The light emitted from the standard LED has several dark spots due to the bonding pad, obstruction from the wire bond as well as the reflector cup . A PSE has a much more narrow, defined, and precise beam with no dark spots.

1.1.2 Expression of Intensity

Intensity is defined as the energy per unit time per unit area.
Which can be expressed as $Intensity = \frac{Engergy}{Time*Area}$
The fraction of $\frac{Energy}{Time}$ is considered as power.
Hence the Intensity can be taken as $Intensity = \frac{Power}{Area}$[31].

As we considered light propagate through free space in all directions taking a shape of spherical wave, we have the expression of Area as $Area = 4\pi r^2$ where r is the radius of the sphere.

Finally intensity may be written as

$$Intensity = \frac{Power}{4\pi r^2} \tag{1.1}$$

If we consider a user a distance of d and if it has multiple intensities from multiple users, the intensity at that user is nothing but the sum of intensities from different users[32].

$$Intensity = I_1 + I_2 + I_3 + ... \tag{1.2}$$

where, I_1 and I_2 are intensities of first and second point sources respectively.

1.2 Arrangement of Point sources considered

Arrangements that are considered in this thesis are as shown in Figure. 1.1

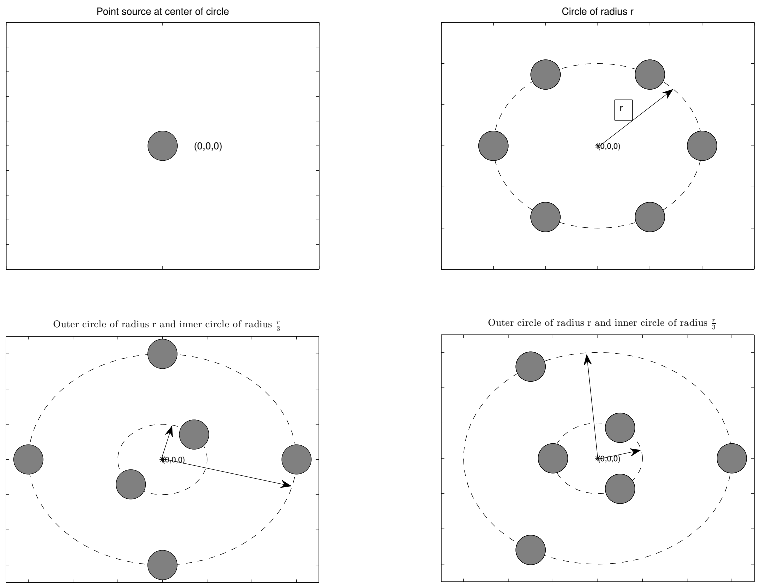

Figure 1.1: System Models considered

- Point source of power P placed at the center of circle at a distance of d from the circle where intensities are been evaluated.
- Six point sources of power $\frac{P}{6}$ placed on the circumference of circle of radius r uniformly.
- Four point sources of power $\frac{P}{6}$ placed on the circumference of circle of radius r and two point sources on circle of radius $\frac{r}{3}$ uniformly.
- Three point sources of power $\frac{P}{6}$ placed on the circumference of circle of radius r and three point sources on the circle of radius $\frac{r}{3}$ uniformly.

1.2.1 Point source placed at the center of the circle

In Figure.1.2 point source with power P is present at the center of the circle and is projecting on to circle of radius R and the distance between the centers of the two circle is d. Consider a small rectangle at a distance of x from the center of the circle of radius of R making an angle of $d\theta$ and has a width of dx. Now the length of the arc becomes $xd\theta$, hence the area of the small rectangular area can be considered as $xdxd\theta$.

We have the expression for the intensity of the light originating from a point at a point present at a distance of a from it as

$$I = \frac{P}{4\pi a^2} \tag{1.3}$$

where,
P is the power of the point sources
a is the distance from the source and the point of observation.

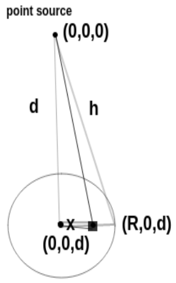

Figure 1.2: Point souce at the center of the circle

Now any point on the circle of radius R at a distance of x from the center can be represented as $(xcos\theta, xsin\theta, d)$ where θ varies between 0 and 2π. Calculating distance between $(0, 0, 0)$ and $(xcos\theta, xsin\theta, d)$ we get

$$distance = \sqrt{(xcos\theta)^2 + (xsin\theta)^2 + d^2} = \sqrt{x^2 + d^2} \tag{1.4}$$

Hence the expression of intensity at any point at a distance of x from the center of the circle of radius R is

$$I1 = \frac{P}{4\pi(d^2 + x^2)} \tag{1.5}$$

Plotting the intensity profile over the circle of radius $R = 5$ where the distance between the centers of circles considered $d = 10$ looks like Figure.1.3

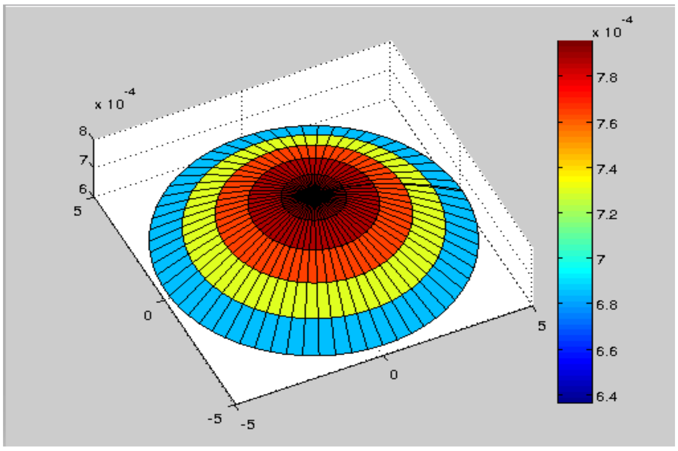

Figure 1.3: Intensity profile with point souce at center of one circle

Now we need to average the expression of intesity over the entire area of the circle of radius R.

This can be calculated as follows

$$I1_{avg} = \frac{1}{\pi R^2} \int_0^{2\pi} \int_0^R \frac{P}{4\pi(d^2 + x^2)} x dx d\theta \tag{1.6}$$

$$\begin{aligned} I1_{avg} &= \frac{1}{\pi R^2}(2\pi)\frac{P}{4\pi} \int_0^R \frac{x}{d^2 + x^2} dx = \frac{P}{4\pi R^2} \int_0^R \frac{2x}{d^2 + x^2} dx \\ &= \frac{P}{4\pi R^2} \left(log(x^2 + d^2)\right)_0^R = \frac{P}{4\pi R^2} \left(log\left(\frac{R^2 + d^2}{d^2}\right)\right) \\ &= \frac{P}{4\pi R^2} log\left(1 + \left(\frac{R}{d}\right)^2\right) \end{aligned} \tag{1.7}$$

Hence the expression in equation (1.7) is the average intensity over area for a point source projecting on to circle of radius R.

Peak to Average Value

We have the expressions of Intensity at any point and average value from equation (1.5) and (1.7) We obtain maximum or peak value at least value of x^2, Hence peak occurs when $x = 0$.

$$I1_{peak} = \frac{P}{4\pi d^2} \tag{1.8}$$

$$\begin{aligned} R1 &= \frac{\frac{P}{4\pi d^2}}{\frac{P}{4\pi R^2} log\left(1 + \left(\frac{R}{d}\right)^2\right)} \\ &= \frac{R^2}{d^2}\left(log\left(1 + \left(\frac{R}{d}\right)^2\right)\right)^{-1} \end{aligned} \tag{1.9}$$

1.2.2 Six point sources on the circumference of the circle of radius r

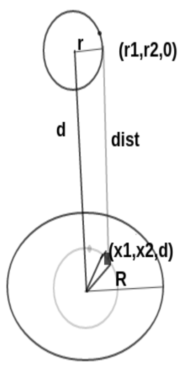

Figure 1.4: Light sources on the circumference of circle of radius r

In Figure.1.4 six point sources of power $\frac{P}{6}$ are placed uniformly on the circumference of circle of radius r and are projected on to circle of radius R and the distance between the two circles is d. Any point on the circumference on the circle of radius r is considered as $(r1, r2, 0)$ where $r1 = rcos\phi$, $r2 = rsin\phi$ and ϕ is the angle where the point source is located. Considering a small area $xdxd\theta$ on the circle of radius R, the coordinates on any such point at a distance of x from the center are $(x1, x2, d)$ where $x1 = xcos\theta$,$x2 = xsin\theta$ and θ is the angle where the point is located on the circle.

Now the intensity expression can be calculated once we know the distance between the point source and the point considered on the circle of radius R. It is nothing but the eucledian distance between $(rcos\phi, rsin\phi, 0)$ and $(xcos\theta, xsin\theta, d)$.

$$\begin{aligned} dist &= \sqrt{(xcos\theta - rcos\phi)^2 + (xsin\theta - rsin\theta)^2 + d^2} \\ &= \sqrt{x^2 + r^2 + d^2 - 2xrcos(\theta - \phi)} \end{aligned}$$

The expression for intensity can be taken as

$$I2 = \sum_{\phi \epsilon \Phi} \frac{P/6}{4\pi(x^2 + r^2 + d^2 - 2xrcos(\theta - \phi))} \tag{1.10}$$

Here ϕ takes values of $\{0, \frac{\pi}{3}, \frac{2\pi}{3}, \frac{3\pi}{3}, \frac{4\pi}{3}, \frac{5\pi}{3}\}$ depending on the point considered on the circumference of the circle and θ takes any value between 0 and 2π depending on the position of the coordinate where the intensity calculation is made.
where, set $\Phi = \{0, \frac{\pi}{3}, \frac{2\pi}{3}, \frac{3\pi}{3}, \frac{4\pi}{3}, \frac{5\pi}{3}\}$
Figure.1.5 was plotted considering $r = 5$,$R = 15$ and $d = 10$. Observing the plot it gives six different

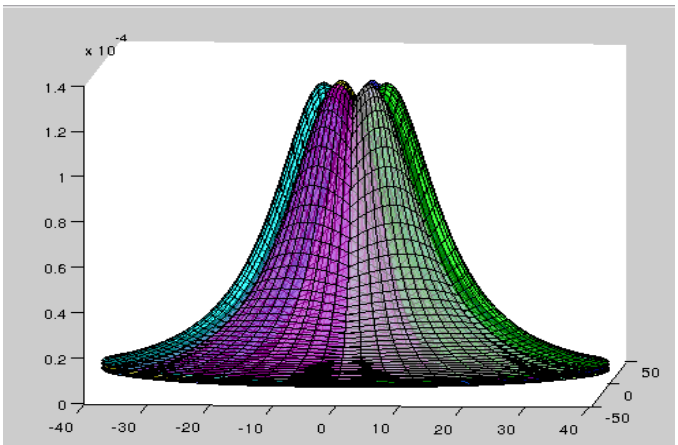

Figure 1.5: Intensity profiles when point sources placed at various ϕ positions

peaks each occuring at the respective ϕ values. The overall intensity profile can be obtained by summing up all these individual profiles.

Figure.1.6 represents the overall intensity profile.
Now we need to calculate the average intensity profile over the entire area of the circle of radius

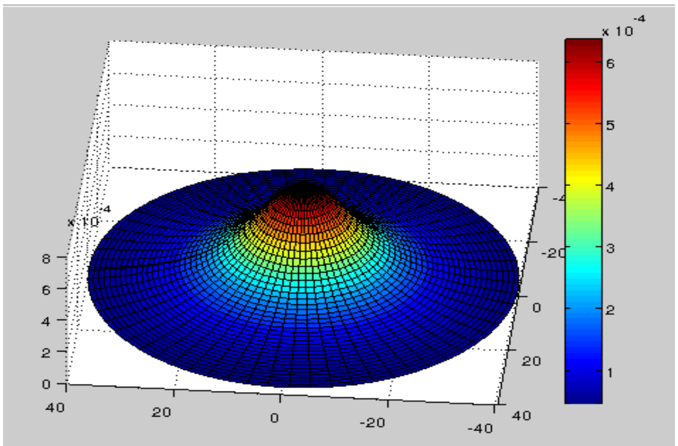

Figure 1.6: Overall Intensity Profile

R.This can be calculated as follows

$$I2_{avg} = \frac{1}{\pi R^2} \sum_{\phi \epsilon \Phi} \int_0^R \int_0^{2\pi} \frac{\frac{P}{6}}{4\pi(x^2 + r^2 + d^2 - 2xrcos(\theta - \phi))} xdxd\theta \tag{1.11}$$

$$\begin{aligned} I2_{avg} &= \frac{1}{\pi R^2} \sum_{\phi \epsilon \Phi} \int_0^R \frac{\frac{P}{6}x}{4\pi} \int_0^{2\pi} \frac{1}{(d^2 + r^2 + x^2) + (-2rxcos(\theta - \phi))} d\theta dx \\ &= \frac{1}{\pi R^2} \sum_{\phi \epsilon \Phi} \int_0^R \frac{\frac{2P}{6}x}{4\pi} \int_0^{\pi} \frac{1}{(d^2 + r^2 + x^2) + (-2rxcos(\theta - \phi))} d\theta dx \\ &= \frac{1}{\pi R^2} \sum_{\phi \epsilon \Phi} \int_0^R \frac{\frac{2P}{6}x}{4\pi} \int_0^{\pi} \frac{d\theta dx}{(d^2 + r^2 + x^2) + (-2rxcos\phi cos\theta - 2xrsin\phi sin\theta)} \end{aligned} \tag{1.12}$$

From [27, (2.558)] in the equation (1.12) $(d^2 + r^2 + x^2)^2 > (-2rx)^2$ and we have the expression for the integral of $\frac{1}{a+bcosx+csinx}$ if $a^2 > b^2 + c^2$ as $\frac{2}{\sqrt{a^2-b^2}} tan^{-1}\left(\frac{(a-b)tan\left(\frac{x}{2}\right)+c}{\sqrt{a^2-b^2-c^2}}\right)$. Substituting the respective value in the equation (1.12) we get

$$\begin{aligned} I2_{avg} = \frac{1}{\pi R^2} \sum_{\phi \epsilon \Phi} \int_0^R \frac{\frac{P}{6}x}{4\pi} \frac{2}{\sqrt{(d^2 + r^2 + x^2)^2 - (2rx)^2}} \times \\ \left(tan^{-1} \left(\frac{((d^2 + r^2 + x^2) + 2rx))tan\left(\frac{\theta}{2}\right) - 2xrsin\phi}{\sqrt{(d^2 + r^2 + x^2)^2 - (2rx)^2}} \right) \right)_0^{2\pi} dx \\ = \frac{1}{\pi R^2} \sum_{\phi \epsilon \Phi} \int_0^R \frac{\frac{P}{6}x}{4\pi} \left(\frac{2}{\sqrt{(d^2 + r^2 + x^2)^2 - (2rx)^2}} \pi \right) dx \end{aligned} \tag{1.13}$$

In the equation (1.13) there is no ϕ term involved hence all the values over the set will just get added up and results the following expression.

$$\begin{aligned} I2_{avg} &= \frac{1}{\pi R^2}\int_0^R \frac{Px}{4\pi}\left(\frac{2}{\sqrt{(d^2+r^2+x^2)^2-(2rx)^2}}\pi\right)dx \\ &= \frac{P}{4\pi R^2}\int_0^R \frac{2x}{\sqrt{(d^2+r^2+x^2)^2-(2rx)^2}}dx \end{aligned} \tag{1.14}$$

Considering $x^2 = t$ in the above expression and rewriting the integral we get,

$$\begin{aligned} I2_{avg} &= \frac{P}{4\pi R^2}\int_0^{R^2} \frac{dt}{\sqrt{t^2+2t(d^2-r^2)+(d^2+r^2)^2}}dt \\ &= \frac{P}{4\pi R^2}\int_0^{R^2} \frac{dt}{\sqrt{(t+(d^2-r^2))^2+(2dr)^2}}dt \end{aligned}$$

We have the integral of $\frac{1}{\sqrt{x^2+a^2}}$ as $log(x+\sqrt{x^2+a^2})$

$$\begin{aligned} I2_{avg} &= \frac{P}{4\pi R^2}\left(log\left((t+(d^2-r^2))+\sqrt{(t+(d^2-r^2))^2+(2dr)^2}\right)\right)_0^{R^2} \\ &= \frac{P}{4\pi R^2}\left(log\left(\frac{R^2+d^2-r^2+\sqrt{(R^2+d^2-r^2)^2+4d^2r^2}}{d^2-r^2+\sqrt{(d^2-r^2)^2+4d^2r^2}}\right)\right) \\ &= \frac{P}{4\pi R^2}\left(log\left(\frac{R^2+d^2-r^2+\sqrt{(R^2+d^2-r^2)^2+4d^2r^2}}{2d^2}\right)\right) \end{aligned} \tag{1.15}$$

Peak to Average Value

We have the expressions for intensity and average intensity from equations (1.10) and (1.15)
We have the peak value of $I2$ when the $cos(\theta-\phi)$ takes a value of 1 and $x=0$ and sum for all six point sources.

$$I2_{peak} = \frac{P}{4\pi(r^2+d^2)} \tag{1.16}$$

Now the ratio of peak to average can be taken as

$$\begin{aligned} R2 &= \frac{\frac{P}{4\pi(r^2+d^2)}}{\frac{P}{4\pi R^2}\left(log\left(\frac{R^2+d^2-r^2+\sqrt{(R^2+d^2-r^2)^2+4d^2r^2}}{2d^2}\right)\right)} \\ &= \frac{R^2}{d^2+r^2}\left(log\left(\frac{R^2+d^2-r^2+\sqrt{(R^2+d^2-r^2)^2+4d^2r^2}}{2d^2}\right)\right)^{-1} \end{aligned} \tag{1.17}$$

1.2.3 Four point sources on the circumference of circle and two at the center

In Figure.1.7 point sources are arranged such that four point sources of power $\frac{P}{6}$ are placed on the circumference of the circle of radius r uniformly and two point sources of same power are placed on a circle of radius $\frac{r}{3}$ uniformly on either side of diameter. The individual intensities of the point

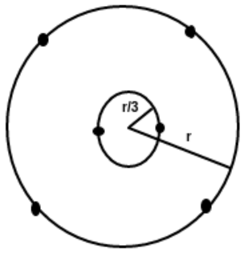

Figure 1.7: Arrangement of point sources on the circle of radius r

sources will be same as that of equation (1.10).
where, for the four point sources on the circumference of circle of circle of radius r the expression is

$$I3_1 = \frac{P/6}{4\pi(x^2 + r^2 + d^2 - 2xrcos(\theta - \phi_1))} \tag{1.18}$$

where, ϕ_1 takes values of $\{\frac{\pi}{4}, \frac{3\pi}{4}, \frac{5\pi}{4}, \frac{7\pi}{4}\}$ and the two point sources placed on the circle of radius $\frac{r}{3}$ takes value of

$$I3_2 = \frac{P/6}{4\pi\left(x^2 + \left(\frac{r}{3}\right)^2 + d^2 - 2x\left(\frac{r}{3}\right)cos(\theta - \phi_2)\right)} \tag{1.19}$$

where,ϕ_2 takes values of $\{0, \pi\}$
Hence the expression of intenisty is given by

$$I3 = \sum_{\phi_1 \epsilon \Phi_1} \frac{P/6}{4\pi(x^2 + r^2 + d^2 - 2xrcos(\theta - \phi_1))} + \sum_{\phi_2 \epsilon \Phi_2} \frac{P/6}{4\pi\left(x^2 + \left(\frac{r}{3}\right)^2 + d^2 - 2x\left(\frac{r}{3}\right)cos(\theta - \phi_2)\right)} \tag{1.20}$$

In Figure.1.8 there are six peaks occuring at six points because of six different positions of point

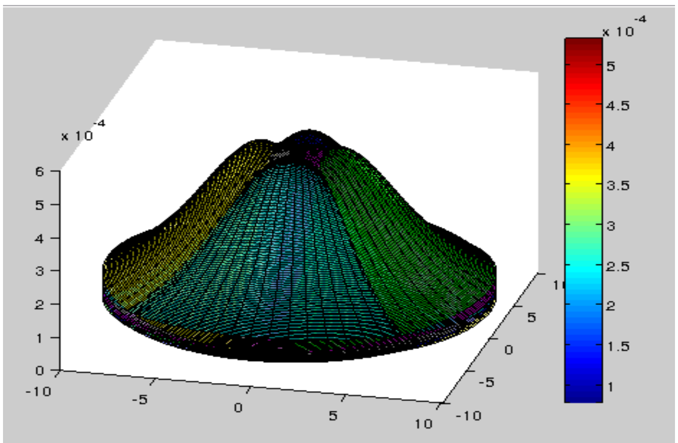

Figure 1.8: Individual intensity profiles

sources that are present. Combining all gives the overall intensity profile over the circle of radius R. Figure.1.9 gives the overall intensity profile summing all the individual intensity profiles.

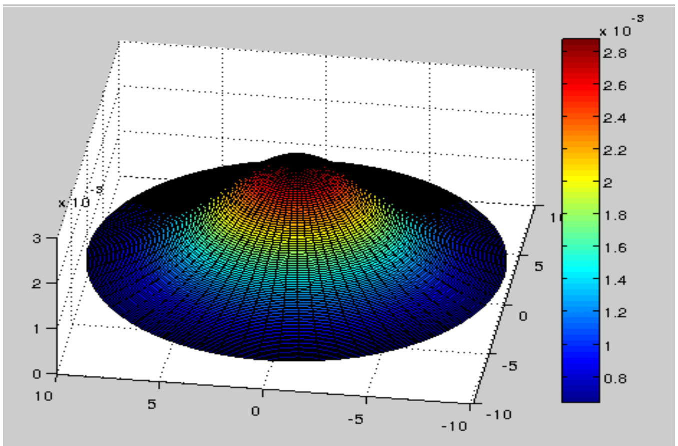

Figure 1.9: Overall Intensity Profile

The average expression for this case may be calculated as follows

$$I3_{avg} = \frac{1}{\pi R^2}\left(\sum_{\phi_1 \epsilon \Phi_1}\int_0^R\int_0^{2\pi} I3_1 dr d\theta + \sum_{\phi_2 \epsilon \Phi_2}\int_0^R\int_0^{2\pi} I3_2 dr d\theta\right)$$

$$I3_{avg} = \frac{1}{\pi R^2}\left(\sum_{\phi_1 \epsilon \Phi_1}\int_0^R\int_0^{2\pi}\frac{P/6}{4\pi(x^2+r^2+d^2-2xrcos(\theta-\phi_1))}dr d\theta\right) + \frac{1}{\pi R^2}\left(\sum_{\phi_2 \epsilon \Phi_2}\int_0^R\int_0^{2\pi}\frac{P/6}{4\pi\left(x^2+\left(\frac{r}{3}\right)^2+d^2-2x\left(\frac{r}{3}\right)cos(\theta-\phi_2)\right)}dr d\theta\right) \quad (1.21)$$

Solving the equation (1.21) we get

$$I3_{avg} = \frac{P}{6\pi R^2}log\left(\frac{R^2+d^2-r^2+\sqrt{(R^2+d^2-r^2)^2+4d^2r^2}}{2d^2}\right) + \frac{P}{12\pi R^2}log\left(\frac{R^2+d^2-(r/3)^2+\sqrt{(R^2+d^2-(r/3)^2)^2+4d^2(r/3)^2}}{2d^2}\right) \quad (1.22)$$

Peak to Average Value

We have the expressions for intensity at any point and average values from equations (1.18),(1.19) and (1.22)

Now the peak value occurs when both cos terms become 1 and $x = 0$ and adding up all the cases

$$I3_{peak} = \frac{P}{24\pi}\left(\frac{4}{r^2+d^2}+\frac{2}{d^2+(r/3)^2}\right) \quad (1.23)$$

Now the ratio of peak to average can be calculated as follows

$$R3 = \frac{\frac{1}{4}\left(\frac{4}{r^2+d^2} + \frac{2}{d^2+(r/3)^2}\right)}{\frac{1}{R^2}log\left(\frac{R^2+d^2-r^2+\sqrt{(R^2+d^2-r^2)^2+4d^2r^2}}{2d^2}\right) + \frac{1}{2R^2}log\left(\frac{R^2+d^2-(r/3)^2+\sqrt{(R^2+d^2-(r/3)^2)^2+4d^2(r/3)^2}}{2d^2}\right)} \tag{1.24}$$

1.2.4 Three point sources on the circumference of outer circle and three on the inner circle

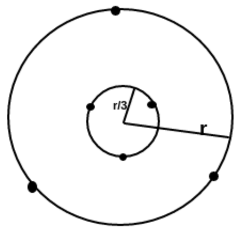

Figure 1.10: Arrangement of point sources on the circle of radius r

In Figure.1.10 point sources are arranged such that three point sources of power $\frac{P}{6}$ are placed on the circumference of the circle of radius r uniformly and three point sources of same power are placed on a circle of radius $\frac{r}{3}$ uniformly. The individual intensities of the point sources will be same as that of equation (1.10).
where, for the three point sources on the circumference of circle of circle of radius r the expression is

$$I4_1 = \frac{P/6}{4\pi(x^2 + r^2 + d^2 - 2xrcos(\theta - \phi_1))} \tag{1.25}$$

where, ϕ_1 takes values of $\{0, \frac{2\pi}{3}, \frac{4\pi}{3}\}$ and the three point sources placed on the circle of radius $\frac{r}{3}$ takes value of

$$I4_2 = \frac{P/6}{4\pi\left(x^2 + \left(\frac{r}{3}\right)^2 + d^2 - 2x\left(\frac{r}{3}\right)cos(\theta - \phi_2)\right)} \tag{1.26}$$

where,ϕ_2 takes values of $\{\frac{\pi}{3}, \pi, \frac{5\pi}{3}\}$
Hence the expression of intenisty is given by

$$I4 = \sum_{\phi_1 \epsilon \Phi_1} \frac{P/6}{4\pi(x^2 + r^2 + d^2 - 2xrcos(\theta - \phi_1))} + \sum_{\phi_2 \epsilon \Phi_2} \frac{P/6}{4\pi\left(x^2 + \left(\frac{r}{3}\right)^2 + d^2 - 2x\left(\frac{r}{3}\right)cos(\theta - \phi_2)\right)} \tag{1.27}$$

In Figure.1.11 there are six peaks occuring at six points because of six different positions of point sources that are present. Combining all gives the overall intensity profile over the circle of radius R. Figure.1.12 gives the overall intensity profile summing all the individual intensity profiles. The average expression for this case may be calculated as follows

$$I4_{avg} = \frac{1}{\pi R^2}\left(\sum_{\phi_1 \epsilon \Phi_1} \int_0^R \int_0^{2\pi} I3_1 dr d\theta + \sum_{\phi_2 \epsilon \Phi_2} \int_0^R \int_0^{2\pi} I3_2 dr d\theta\right)$$

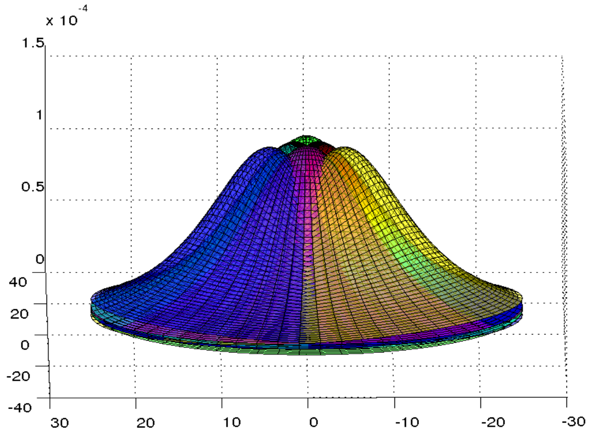

Figure 1.11: Individual intensity profiles

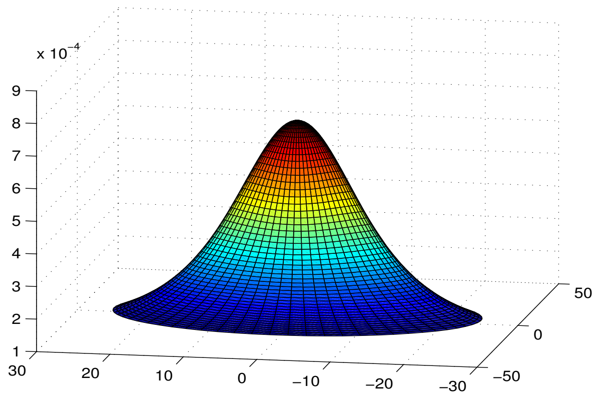

Figure 1.12: Overall Intensity Profile

$$I4_{avg} = \frac{1}{\pi R^2}\left(\sum_{\phi_1 \epsilon \Phi_1}\int_0^R\int_0^{2\pi}\frac{P/6}{4\pi(x^2+r^2+d^2-2xrcos(\theta-\phi_1))}drd\theta\right)+ \frac{1}{\pi R^2}\left(\sum_{\phi_2 \epsilon \Phi_2}\int_0^R\int_0^{2\pi}\frac{P/6}{4\pi\left(x^2+\left(\frac{r}{3}\right)^2+d^2-2x\left(\frac{r}{3}\right)cos(\theta-\phi_2)\right)}drd\theta\right) \quad (1.28)$$

Solving the equation (1.28) we get

$$I3_{avg} = \frac{P}{8\pi R^2}log\left(\frac{R^2+d^2-r^2+\sqrt{(R^2+d^2-r^2)^2+4d^2r^2}}{2d^2}\right) + \frac{P}{8\pi R^2}log\left(\frac{R^2+d^2-(r/3)^2+\sqrt{(R^2+d^2-(r/3)^2)^2+4d^2(r/3)^2}}{2d^2}\right) \quad (1.29)$$

Peak to Average Value

We have the expressions for intensity at any point and average values from equations (1.25),(1.26) and (1.29)
Now the peak value occurs when both cos terms become 1 and $x = 0$ and adding up all the cases

$$I4_{peak} = \frac{P}{8\pi}\left(\frac{1}{r^2+d^2} + \frac{1}{d^2+(r/3)^2}\right) \tag{1.30}$$

Now the ratio of peak to average can be calculated as follows

$$R4 = \frac{\left(\frac{1}{r^2+d^2} + \frac{1}{d^2+(r/3)^2}\right)}{\frac{1}{R^2}log\left(\frac{R^2+d^2-r^2+\sqrt{(R^2+d^2-r^2)^2+4d^2r^2}}{2d^2}\right) + \frac{1}{R^2}log\left(\frac{R^2+d^2-(r/3)^2+\sqrt{(R^2+d^2-(r/3)^2)^2+4d^2(r/3)^2}}{2d^2}\right)} \tag{1.31}$$

1.3 Comparisions between all the arrangements considered

1.3.1 Relation between d, R and r so that case 2 perform better than case 1 beyond radius R_1

Considering expressions of average intensity of first and second cases i.e., a point source present at the center and six point sources placed on the circumference of the circle.

Here we derive an expression for distance between the source and destination and the radius R_1 after which the case 2 performs better.

Considering two circles of radius R_1 and R and we consider the average intensity obtained in first case should be less than the average intensity of second case since case 2 performs better in this region.
We have the expressions of average intensities of both cases in that region as

$$I1_{avg} = \frac{P}{4\pi(R^2-R_1^2)}log\left(\frac{R^2+d^2}{R_1^2+d^2}\right)$$
$$I2_{avg} = \frac{P}{4\pi(R^2-R_1^2)}log\left(\frac{R^2+d^2-r^2+\sqrt{(R^2+d^2+r^2)^2+(2dr)^2}}{R_1^2+d^2-r^2+\sqrt{(R_1^2+d^2+r^2)^2+(2dr)^2}}\right)$$

Now the relation between $I1_{avg}$ and $I2_{avg}$ should be $I1_{avg} < I2_{avg}$.

$$\frac{P}{4\pi(R^2-R_1^2)}log\left(\frac{R^2+d^2}{R_1^2+d^2}\right) < \frac{P}{4\pi(R^2-R_1^2)}log\left(\frac{R^2+d^2-r^2+\sqrt{(R^2+d^2-r^2)^2+(2dr)^2}}{R_1^2+d^2-r^2+\sqrt{(R_1^2+d^2-r^2)^2+(2dr)^2}}\right)$$

$$log\left(\frac{R^2+d^2}{R_1^2+d^2}\right) < log\left(\frac{R^2+d^2-r^2+\sqrt{(R^2+d^2-r^2)^2+(2dr)^2}}{R_1^2+d^2-r^2+\sqrt{(R_1^2+d^2-r^2)^2+(2dr)^2}}\right)$$

$$\left(\frac{R^2+d^2}{R_1^2+d^2}\right) < \left(\frac{R^2+d^2-r^2+\sqrt{(R^2+d^2-r^2)^2+(2dr)^2}}{R_1^2+d^2-r^2+\sqrt{(R_1^2+d^2-r^2)^2+(2dr)^2}}\right)$$

$$(R^2+d^2)(R_1^2+d^2-r^2+\sqrt{(R_1^2+d^2-r^2)^2+(2dr)^2}) < (R_1^2+d^2)(R^2+d^2-r^2+\sqrt{(R^2+d^2-r^2)^2+(2dr)^2})$$

$$R_1^2r^2 \ + \ (R^2+d^2)\sqrt{(R_1^2+d^2-r^2)^2+(2dr)^2} \ < \ R^2r^2 \ + \ (R_1^2+d^2)\sqrt{(R^2+d^2-r^2)^2+(2dr)^2}$$

Now expressing R_1,d and R in terms of r, as

$$d = \alpha r$$
$$R_1 = \beta r$$
$$R = \gamma r$$

Rewriting the above equation we get.,

$$\beta^2 + (\gamma^2+\alpha^2)\sqrt{(\beta^2+\alpha^2-1)^2+4\alpha^2} < \gamma^2 + (\beta^2+\alpha^2)\sqrt{(\gamma^2+\alpha^2-1)^2+4\alpha^2} \quad (1.32)$$

We already know the value of γ since the relation between r and R is known.
Now fixing either of the values of β or α we will get the relation of other.

1.3.2 Average intensities of case 3 and case 4 are always greater than case 2

$I2_{avg} < I3_{avg}$**:**

Let us consider case 3 performs over case 2 over a radius of R_1.
Hence the average intensity over radius of R_1 of case 3 should be greater than that of the average intensity of case 2.

$$\frac{P}{4\pi(R_1^2)}log\left(\frac{R_1^2+d^2-r^2+\sqrt{(R_1^2+d^2-r^2)^2+(2dr)^2}}{2d^2}\right) < \frac{P}{6\pi(R_1^2)}log\left(\frac{R_1^2+d^2-r^2+\sqrt{(R_1^2+d^2-r^2)^2+(2dr)^2}}{2d^2}\right) + \frac{P}{12\pi(R_1^2)}log\left(\frac{R_1^2+d^2-\left(\frac{r}{3}\right)^2+\sqrt{(R_1^2+d^2-\left(\frac{r}{3}\right)^2)^2+(2d\frac{r}{3})^2}}{2d^2}\right)$$

$$\frac{P \times log\left(\frac{R_1^2+d^2-r^2+\sqrt{(R_1^2+d^2-r^2)^2+(2dr)^2}}{2d^2}\right)}{12\pi(R_1^2)} < \frac{P \times log\left(\frac{R_1^2+d^2-\left(\frac{r}{3}\right)^2+\sqrt{(R_1^2+d^2-\left(\frac{r}{3}\right)^2)^2+(2d\frac{r}{3})^2}}{2d^2}\right)}{12\pi(R_1^2)}$$

$$log\left(\frac{R_1^2+d^2-r^2+\sqrt{(R_1^2+d^2-r^2)^2+(2dr)^2}}{2d^2}\right) < log\left(\frac{R_1^2+d^2-\left(\frac{r}{3}\right)^2+\sqrt{(R_1^2+d^2-\left(\frac{r}{3}\right)^2)^2+(2d\frac{r}{3})^2}}{2d^2}\right) \tag{1.33}$$

$I2_{avg} < I4_{avg}$**:**

Let us consider case 4 performs over case 2 over a radius of R_1.
Hence the average intensity over radius of R_1 of case 4 should be greater than that of the average intensity of case 2.

$$\frac{P}{4\pi(R_1^2)} log\left(\frac{R_1^2+d^2-r^2+\sqrt{(R_1^2+d^2-r^2)^2+(2dr)^2}}{2d^2}\right) < \frac{P}{8\pi(R_1^2)} log\left(\frac{R_1^2+d^2-r^2+\sqrt{(R_1^2+d^2-r^2)^2+(2dr)^2}}{2d^2}\right) + \frac{P}{8\pi(R_1^2)} log\left(\frac{R_1^2+d^2-\left(\frac{r}{3}\right)^2+\sqrt{(R_1^2+d^2-\left(\frac{r}{3}\right)^2)^2+(2d\frac{r}{3})^2}}{2d^2}\right)$$

$$\frac{P \times log\left(\frac{R_1^2+d^2-r^2+\sqrt{(R_1^2+d^2-r^2)^2+(2dr)^2}}{2d^2}\right)}{8\pi(R_1^2)} < \frac{P \times log\left(\frac{R_1^2+d^2-\left(\frac{r}{3}\right)^2+\sqrt{(R_1^2+d^2-\left(\frac{r}{3}\right)^2)^2+(2d\frac{r}{3})^2}}{2d^2}\right)}{8\pi(R_1^2)}$$

$$log\left(\frac{R_1^2+d^2-r^2+\sqrt{(R_1^2+d^2-r^2)^2+(2dr)^2}}{2d^2}\right) < log\left(\frac{R_1^2+d^2-\left(\frac{r}{3}\right)^2+\sqrt{(R_1^2+d^2-\left(\frac{r}{3}\right)^2)^2+(2d\frac{r}{3})^2}}{2d^2}\right) \tag{1.34}$$

In both the cases the expressions in 1.33 and 1.34 are the same and can be solved as follows,

$$\left(\frac{R_1^2+d^2-r^2+\sqrt{(R_1^2+d^2-r^2)^2+(2dr)^2}}{2d^2}\right) < \left(\frac{R_1^2+d^2-\left(\frac{r}{3}\right)^2+\sqrt{(R_1^2+d^2-\left(\frac{r}{3}\right)^2)^2+(2d\frac{r}{3})^2}}{2d^2}\right)$$

$$R_1^2+d^2-r^2+\sqrt{(R_1^2+d^2-r^2)^2+(2dr)^2} < R_1^2+d^2-\left(\frac{r}{3}\right)^2+\sqrt{\left(R_1^2+d^2-\left(\frac{r}{3}\right)^2\right)^2+(2d\frac{r}{3})^2}$$

$$\sqrt{(R_1^2+d^2-r^2)^2+(2dr)^2} < \frac{8r^2}{9}+\sqrt{\left(R_1^2+d^2-\left(\frac{r}{3}\right)^2\right)^2+\left(2d\frac{r}{3}\right)^2}$$

Now considering all variables in terms of r as follows,

$$R_1 = \beta r$$
$$d = \alpha r$$

$$\sqrt{(\beta^2+\alpha^2-1)^2+4\alpha^2} < \frac{8}{9}+\sqrt{\left(\beta^2+\alpha^2-\frac{1}{9}\right)^2+\frac{4\alpha^2}{9}}$$

Squaring on both sides

$$(\beta^2+\alpha^2-1)^2+4\alpha^2 < \frac{64}{81}+(\beta^2+\alpha^2-\frac{1}{9})^2+\frac{4\alpha^2}{9}+\frac{16}{9}\sqrt{(\beta^2+\alpha^2-\frac{1}{9})^2+\frac{4\alpha^2}{9}}$$
$$1-2(\alpha^2+\beta^2)+4\alpha^2 < \frac{65}{81}-\frac{2}{9}(\alpha^2+\beta^2)+\frac{4\alpha^2}{9}+\frac{16}{9}\sqrt{(\beta^2+\alpha^2-\frac{1}{9})^2+\frac{4\alpha^2}{9}}$$

$$\frac{16}{81}-\frac{16}{9}(\beta^2-\alpha^2) < \frac{16}{9}\sqrt{(\beta^2+\alpha^2-\frac{1}{9})^2+\frac{4\alpha^2}{9}}$$
$$\frac{1}{9}-\beta^2+\alpha^2 < \sqrt{(\beta^2+\alpha^2-\frac{1}{9})^2+\frac{4\alpha^2}{9}}$$

Again squaring on both sides

$$\left(\alpha^2-\left(\beta^2-\frac{1}{9}\right)\right)^2 < \left(\left(\beta^2-\frac{1}{9}\right)+\alpha^2\right)^2+\frac{4\alpha^2}{9}$$
$$-2\alpha^2\left(\beta^2-\frac{1}{9}\right) < 2\alpha^2\left(\beta^2-\frac{1}{9}\right)+\frac{4\alpha^2}{9}$$
$$-2\alpha^2\beta^2 < 2\alpha^2\beta^2$$
$$\alpha^2\beta^2 > 0 \tag{1.35}$$

Hence from equation (1.35) which is always true, irrespective of the values of α and β average values in case 3 and case 4 are always greater than the average value in case 2.

1.3.3 Relation between d,R and r so that case 3 has higher coverage than case 1 beyond radius R_1

Let $I1_{avg}$ is the average value of intensity for case 1 over the annulus between radius R and radius R_1 and $I3_{avg}$ is the corresponding average.

$$\frac{P}{4\pi(R^2-{R_1}^2)}log\left(\frac{R^2+d^2}{R_1^2+d^2}\right) < \frac{P}{6\pi(R^2-{R_1}^2)}log\left(\frac{R^2+d^2-r^2+\sqrt{(R^2+d^2-r^2)^2+(2dr)^2}}{R_1^2+d^2-r^2+\sqrt{(R_1^2+d^2-r^2)^2+(2dr)^2}}\right)$$
$$+\frac{P}{12\pi(R^2-{R_1}^2)}log\left(\frac{R^2+d^2-\left(\frac{r}{3}\right)^2+\sqrt{(R^2+d^2-\left(\frac{r}{3}\right)^2)^2+(2d\left(\frac{r}{3}\right))^2}}{R_1^2+d^2-\left(\frac{r}{3}\right)^2+\sqrt{(R_1^2+d^2-\left(\frac{r}{3}\right)^2)^2+(2d\left(\frac{r}{3}\right))^2}}\right)$$

$$\frac{1}{2}log\left(\frac{R^2+d^2}{R_1^2+d^2}\right) < \frac{1}{3}log\left(\frac{R^2+d^2-r^2+\sqrt{(R^2+d^2-r^2)^2+(2dr)^2}}{R_1^2+d^2-r^2+\sqrt{(R_1^2+d^2-r^2)^2+(2dr)^2}}\right)$$
$$+\frac{1}{6}log\left(\frac{R^2+d^2-\left(\frac{r}{3}\right)^2+\sqrt{(R^2+d^2-\left(\frac{r}{3}\right)^2)^2+(2d\left(\frac{r}{3}\right))^2}}{R_1^2+d^2-\left(\frac{r}{3}\right)^2+\sqrt{(R_1^2+d^2-\left(\frac{r}{3}\right)^2)^2+(2d\left(\frac{r}{3}\right))^2}}\right)$$

$$\left(\frac{R^2+d^2}{R_1^2+d^2}\right)^{\frac{1}{2}} < \left(\frac{R^2+d^2-r^2+\sqrt{(R^2+d^2-r^2)^2+(2dr)^2}}{R_1^2+d^2-r^2+\sqrt{(R_1^2+d^2-r^2)^2+(2dr)^2}}\right)^{\frac{1}{3}} \left(\frac{R^2+d^2-\left(\frac{r}{3}\right)^2+\sqrt{(R^2+d^2-\left(\frac{r}{3}\right)^2)^2+(2d\left(\frac{r}{3}\right))^2}}{R_1^2+d^2-\left(\frac{r}{3}\right)^2+\sqrt{(R_1^2+d^2-\left(\frac{r}{3}\right)^2)^2+(2d\left(\frac{r}{3}\right))^2}}\right)^{\frac{1}{6}}$$

Introducing a power of 6 on both sides

$$\left(\frac{R^2+d^2}{R_1^2+d^2}\right)^{3} < \left(\frac{R^2+d^2-r^2+\sqrt{(R^2+d^2-r^2)^2+(2dr)^2}}{R_1^2+d^2-r^2+\sqrt{(R_1^2+d^2-r^2)^2+(2dr)^2}}\right)^{2} \times \left(\frac{R^2+d^2-\left(\frac{r}{3}\right)^2+\sqrt{(R^2+d^2-\left(\frac{r}{3}\right)^2)^2+(2d\left(\frac{r}{3}\right))^2}}{R_1^2+d^2-\left(\frac{r}{3}\right)^2+\sqrt{(R_1^2+d^2-\left(\frac{r}{3}\right)^2)^2+(2d\left(\frac{r}{3}\right))^2}}\right)$$

Now writing all the values in terms of r as follows

$$d = \alpha r$$
$$R_1 = \beta r$$
$$R = \gamma r$$

We get,

$$\left(\frac{\gamma^2+\alpha^2}{\beta^2+\alpha^2}\right)^{3} < \left(\frac{\gamma^2+\alpha^2-1+\sqrt{(\alpha^2+\gamma^2-1)^2+4\alpha^2}}{\beta^2+\alpha^2-1+\sqrt{(\alpha^2+\beta^2-1)^2+4\alpha^2}}\right)^{2} \left(\frac{\gamma^2+\alpha^2-\frac{1}{9}+\sqrt{(\alpha^2+\gamma^2-\frac{1}{9})^2+\frac{4\alpha^2}{9}}}{\beta^2+\alpha^2-\frac{1}{9}+\sqrt{(\alpha^2+\beta^2-\frac{1}{9})^2+\frac{4\alpha^2}{9}}}\right)$$

We already have the value of γ since we know the relation between r and R, substituting either of the value of α or β the relation of other can be obtained.

1.3.4 Relation between d,R and r so that case 4 has higher coverage than case 1 beyond radius R_1

Let $I1_{avg}$ is the average value of intensity for case 1 over the annulus between radius R and radius R_1 and $I4_{avg}$ is the corresponding average.

$$\frac{P}{4\pi(R^2-{R_1}^2)} log\left(\frac{R^2+d^2}{R_1^2+d^2}\right) < \frac{P}{8\pi(R^2-{R_1}^2)} log\left(\frac{R^2+d^2-r^2+\sqrt{(R^2+d^2-r^2)^2+(2dr)^2}}{R_1^2+d^2-r^2+\sqrt{(R_1^2+d^2-r^2)^2+(2dr)^2}}\right) + \frac{P}{8\pi(R^2-{R_1}^2)} log\left(\frac{R^2+d^2-\left(\frac{r}{3}\right)^2+\sqrt{(R^2+d^2-\left(\frac{r}{3}\right)^2)^2+(2d\left(\frac{r}{3}\right))^2}}{R_1^2+d^2-\left(\frac{r}{3}\right)^2+\sqrt{(R_1^2+d^2-\left(\frac{r}{3}\right)^2)^2+(2d\left(\frac{r}{3}\right))^2}}\right)$$

$$log\left(\frac{R^2+d^2}{R_1^2+d^2}\right) < \frac{1}{2} log\left(\frac{R^2+d^2-r^2+\sqrt{(R^2+d^2-r^2)^2+(2dr)^2}}{R_1^2+d^2-r^2+\sqrt{(R_1^2+d^2-r^2)^2+(2dr)^2}}\right) + \frac{1}{2} log\left(\frac{R^2+d^2-\left(\frac{r}{3}\right)^2+\sqrt{(R^2+d^2-\left(\frac{r}{3}\right)^2)^2+(2d\left(\frac{r}{3}\right))^2}}{R_1^2+d^2-\left(\frac{r}{3}\right)^2+\sqrt{(R_1^2+d^2-\left(\frac{r}{3}\right)^2)^2+(2d\left(\frac{r}{3}\right))^2}}\right)$$

$$\left(\frac{R^2+d^2}{R_1^2+d^2}\right) < \left(\frac{R^2+d^2-r^2+\sqrt{(R^2+d^2-r^2)^2+(2dr)^2}}{R_1^2+d^2-r^2+\sqrt{(R_1^2+d^2-r^2)^2+(2dr)^2}}\right)^{\frac{1}{2}} \left(\frac{R^2+d^2-\left(\frac{r}{3}\right)^2+\sqrt{(R^2+d^2-\left(\frac{r}{3}\right)^2)^2+(2d\left(\frac{r}{3}\right))^2}}{R_1^2+d^2-\left(\frac{r}{3}\right)^2+\sqrt{(R_1^2+d^2-\left(\frac{r}{3}\right)^2)^2+(2d\left(\frac{r}{3}\right))^2}}\right)^{\frac{1}{2}}$$

Introducing a power of 2 on both sides

$$\left(\frac{R^2+d^2}{R_1^2+d^2}\right)^2 < \left(\frac{R^2+d^2-r^2+\sqrt{(R^2+d^2-r^2)^2+(2dr)^2}}{R_1^2+d^2-r^2+\sqrt{(R_1^2+d^2-r^2)^2+(2dr)^2}}\right) \times \left(\frac{R^2+d^2-\left(\frac{r}{3}\right)^2+\sqrt{(R^2+d^2-\left(\frac{r}{3}\right)^2)^2+(2d\left(\frac{r}{3}\right))^2}}{R_1^2+d^2-\left(\frac{r}{3}\right)^2+\sqrt{(R_1^2+d^2-\left(\frac{r}{3}\right)^2)^2+(2d\left(\frac{r}{3}\right))^2}}\right)$$

Now writing all the values in terms of r as follows

$$d = \alpha r$$
$$R_1 = \beta r$$
$$R = \gamma r$$

We get,

$$\left(\frac{\gamma^2+\alpha^2}{\beta^2+\alpha^2}\right)^2 < \left(\frac{\gamma^2+\alpha^2-1+\sqrt{(\alpha^2+\gamma^2-1)^2+4\alpha^2}}{\beta^2+\alpha^2-1+\sqrt{(\alpha^2+\beta^2-1)^2+4\alpha^2}}\right) \left(\frac{\gamma^2+\alpha^2-\frac{1}{9}+\sqrt{(\alpha^2+\gamma^2-\frac{1}{9})^2+\frac{4\alpha^2}{9}}}{\beta^2+\alpha^2-\frac{1}{9}+\sqrt{(\alpha^2+\beta^2-\frac{1}{9})^2+\frac{4\alpha^2}{9}}}\right)$$

We already have the value of γ since we know the relation between r and R, substituting either of the value of α or β the relation of other can be obtained.

1.3.5 Average intensity of case 4 is always greater than case 3

Let us consider case 4 performs over case 3 over a radius of R_1.
Hence the average intensity over radius of R_1 of case 4 should be greater than that of the average intensity of case 3.

$$\frac{P}{6\pi R_1^2} log\left(\frac{R_1^2+d^2-r^2+\sqrt{(R_1^2+d^2-r^2)^2+(2dr)^2}}{2d^2}\right) + \frac{P}{12\pi R_1^2} log\left(\frac{R_1^2+d^2-\left(\frac{r}{3}\right)^2+\sqrt{(R_1^2+d^2-\left(\frac{r}{3}\right)^2)^2+(2d\frac{r}{3})^2}}{2d^2}\right)$$
$$< \frac{P}{8\pi R_1^2} log\left(\frac{R_1^2+d^2-r^2+\sqrt{(R_1^2+d^2-r^2)^2+(2dr)^2}}{2d^2}\right) + \frac{P}{8\pi R_1^2} log\left(\frac{R_1^2+d^2-\left(\frac{r}{3}\right)^2+\sqrt{(R_1^2+d^2-\left(\frac{r}{3}\right)^2)^2+(2d\frac{r}{3})^2}}{2d^2}\right) \quad (1.36)$$

$$\frac{P}{24\pi R_1^2} log\left(\frac{R_1^2+d^2-r^2+\sqrt{(R_1^2+d^2-r^2)^2+(2dr)^2}}{2d^2}\right) < \frac{P}{24\pi R_1^2} log\left(\frac{R_1^2+d^2-\left(\frac{r}{3}\right)^2+\sqrt{(R_1^2+d^2-\left(\frac{r}{3}\right)^2)^2+(2d\frac{r}{3})^2}}{2d^2}\right)$$
$$\left(\frac{R_1^2+d^2-r^2+\sqrt{(R_1^2+d^2-r^2)^2+(2dr)^2}}{2d^2}\right) < \left(\frac{R_1^2+d^2-\left(\frac{r}{3}\right)^2+\sqrt{(R_1^2+d^2-\left(\frac{r}{3}\right)^2)^2+(2d\frac{r}{3})^2}}{2d^2}\right) \quad (1.37)$$

This expression is same as that in 1.33 hence is true for any value of R_1.

1.4 Metric that defines best case

Following metrics are considered to define the best case

- Coverage
- Average intensity

Some of the considerations that are to be made during the selection of a particular case are
Peak to average value should be as low as possible. Only then the distribution will be flat else at the edges the value will be very low compared to that at the center.
At the same time the average value should be comparable with that of the average value when a single point source is placed at the center of the circle of radius r.

Considering the expressions from the comparisions made in the above section, we prove the coverage of single point source is less when compared to case where six point sources present on the circumference of the circle.

Also the average value of case 4 ie., case where three point sources are placed on the outer circle and three on the inner circle is better compared to case 2 ie., case where all six point sources placed on the circumference of the outer circle.

1.5 Results and Discussion

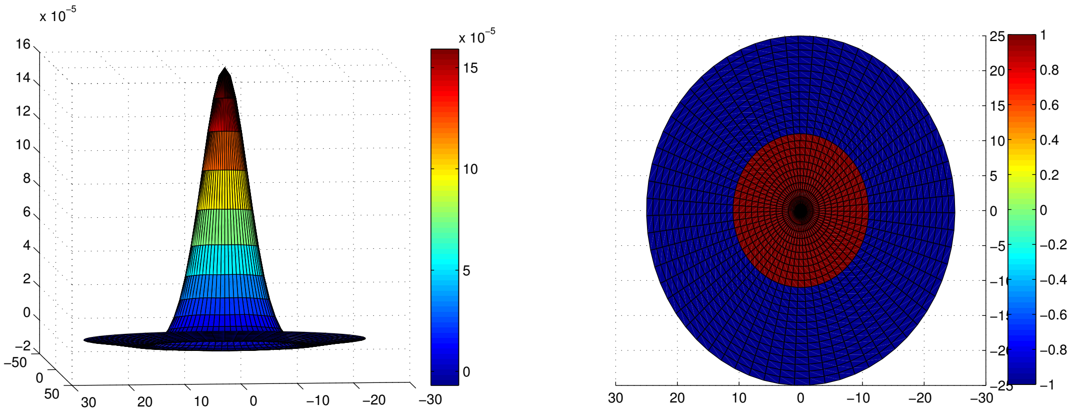

(a) Difference plot (b) Sign of difference plot

Figure 1.13: Comparing case 1 and case 2

Observing the plots in Figure. 1.13 we observe that the coverage is high for case 2 compared to that of case1 ie., the point source. At the center over some radius point source perform better, where as over the remaining annulus case where point sources placed on the circumference perform better.

Similarly observing plots in Figure. 1.14 and 1.15 we observe the coverage in both the cases ie., case 3 and case 4 is higher compared to that of point sources.

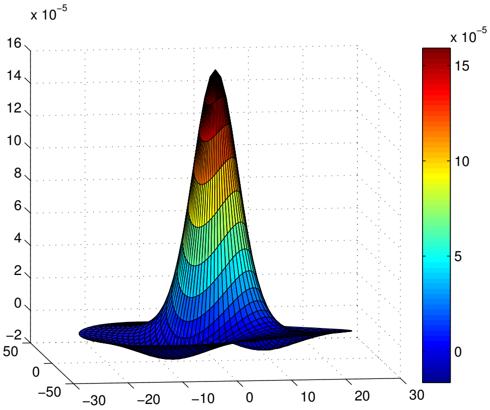

(a) Difference plot

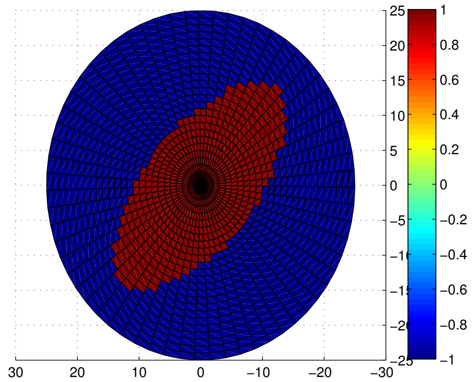

(b) Sign of difference plot

Figure 1.14: Comparing case 1 and case 3

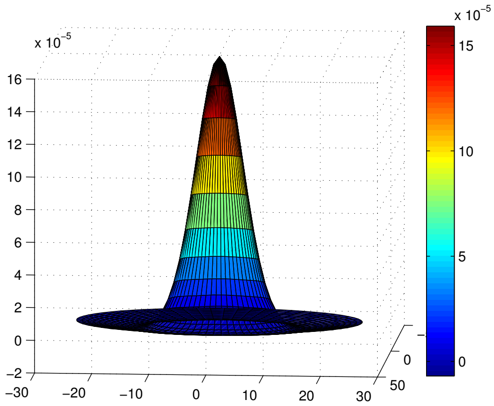

(a) Difference plot

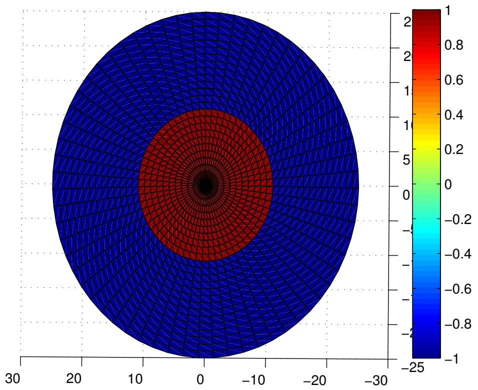

(b) Sign of difference plot

Figure 1.15: Comparing case 1 and case 4

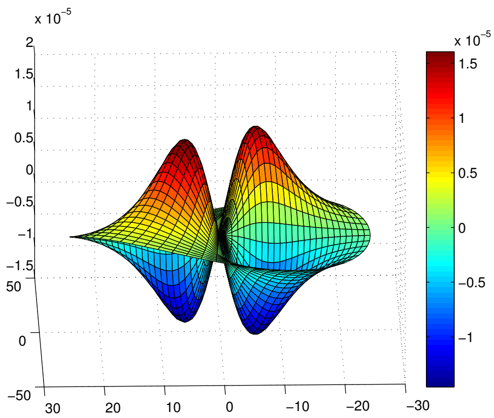

(a) Difference plot

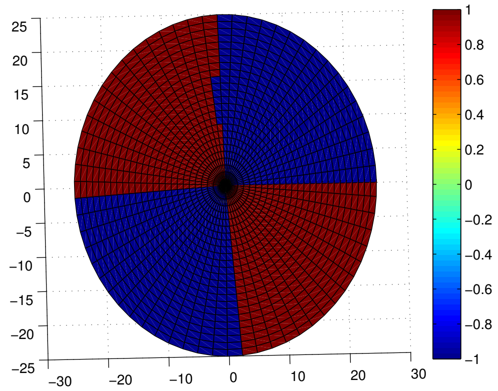

(b) Sign of difference plot

Figure 1.16: Comparing case 2 and case 3

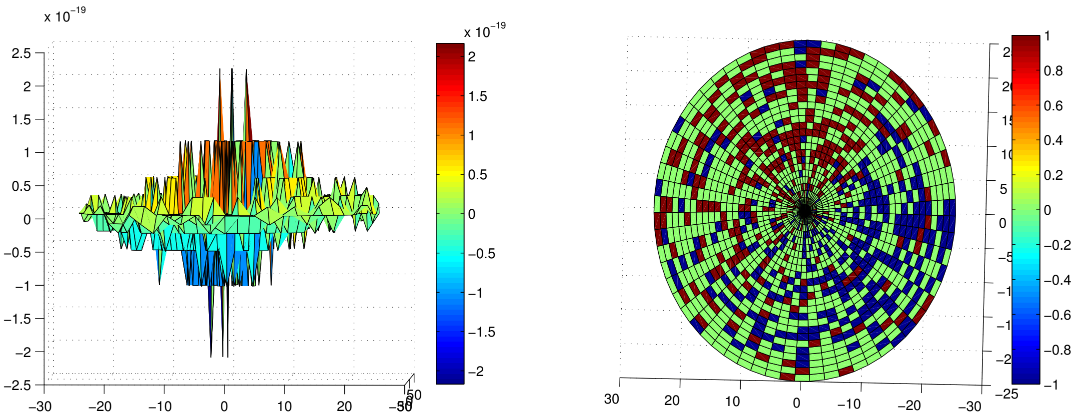

(a) Difference plot (b) Sign of difference plot

Figure 1.17: Comparing case 2 and case 4

Now observering plots in Figure. 1.16 placing two point sources in the inner circle will improve the intensity in some parts of the projection plane but not in other places.

Also from Figure. 1.17 we observe that there is improvement in some parts of the plane.

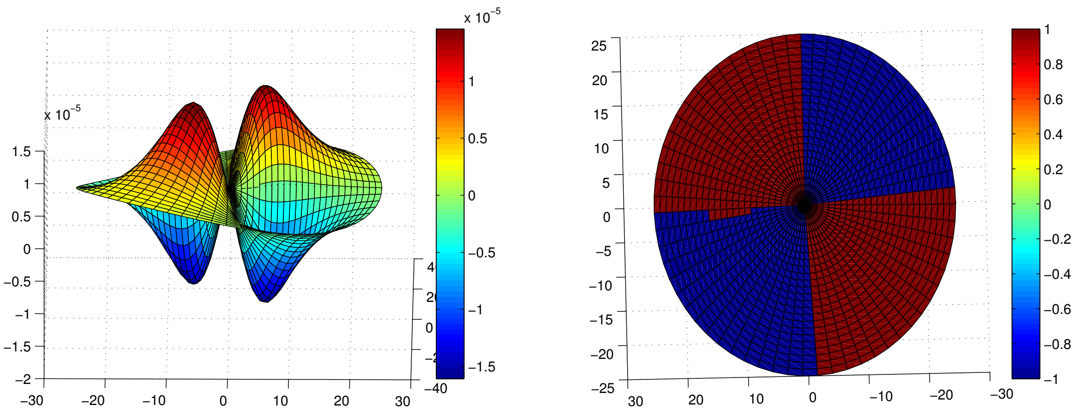

(a) Difference plot (b) Sign of difference plot

Figure 1.18: Comparing case 3 and case 4

Finally, observing plot in Figure. 1.18 there is improvement in one portion of the plot.

Through all the above mentioned plots coverage is being defined. Plot were drawn considering $P = 1$ in all the aforementioned plots.

Other metric in our consideration is to have comparable average intensity along with coverage.

Considering average values for various cases from the Table 1.1 we observe the average values in case 4 ie., case where three point sources place in inner circle has better values comparable with that of point source.

Also the coverage is better with this case. Hence case where three point sources placed on circumference of inner circle and three on the outer circumference performs over all the other cases.

Table 1.1: Average intensity over area for various values of R,d,r

r	R	d	case 1	case 2	case 3	case 4
5	5r	10	0.0908	0.0894	0.0898	0.0900
5	3r	10	0.1501	0.1433	0.1453	0.1463
5	3r	15	0.0883	0.0848	0.0858	0.0863
5	5r	15	0.0609	0.0599	0.0602	0.0604
2	5r	10	0.1986	0.1957	0.1966	0.1970
2	5r	5	0.4611	0.4537	0.4559	0.4570

1.6 Conclusion

Hence placing point sources on the circumference improves the coverage area of the point sources when compared to a point source placed at the center of the circle. Where as the intensity at the center of the region where all the point sources are projecting, will be low for the case where point sources are placed on the circumference compared to a point source at the center.

To improve this we can place three point sources on the circumference of the circle and three on the circumference of the inner circle uniformly. This improves performance at the center compared to all point sources placed on the circumference case. It will degrade the performance at the edges compared to case where all point sources placed on the circumference but not as much as where a point source placed at the center of circle.

Chapter 2

Geometry and Coverage analysis for LED sources

2.1 Introduction

In the recent days with the development of high brightness LEDs there was a change in the lighing world.LEDs are being replaced with the convensional light sources in almost all the applications[11]-[13]. Many efforts were made to achive uniform illuminanace over a planar surface by increasing the source-to-target distance [14]-[19]. In all these techniques irradiance distributions of the LEDs are being merged to produce uniform distribution on planar surfaces. Many research's were made on arrangement of these LEDs to achive uniform distribution as one LED may not give sufficient brightness. Moreno proposed a method for optimizing LED-to-LED spac- ing to achieve uniform irradiance by considering each LED as an imperfect Lambertian source [20]. Freeform lens with large view angle for LED uniform illumination was considered in [21]. Many similar arrangements were considered in [22]-[25] In all the mentioned techniques they have considered a plane of sources that is parallel to the plane where illuminance is measured.In this thesis we consider a circular space of radius r which has point sources of light projecting on to a cicular surface of radius R placed in parallel to the source circle at a distance of d. Here we are evaluating the geometrical arrangement which gives better coverage and average intensity comparably. We have considered peak to average ratio as a metric to evaluate the perfomance of all the arrangements considered.

Light is a electromagnetic wave that propagate through free space. In free space communications we consider there is nothing between the transmitter and the receiver [28]-[29] and the light travels with the speed of light. Light originating from free space take a spherical shape and propagate in all directions since it is isotrpic. Hence the intensity vary at different instants of time depending on the radius.Therefore the distance between the source and the incident point also have high importance[30].

2.1.1 Expression of irradiance

Practical approximation of irradiance distribution may be considered as

$$E(r) = E_o(r)cos^m\xi \tag{2.1}$$

where, ξ is the viewing angle and m is a number that depends on the LED considered.

m can be taken as $\frac{-ln2}{ln(cos\xi_{1/2})}$ and m can take a value of greater than 30.

where, $\xi_{1/2}$ is the view angle when irradiance is half of the value at 0^o.

Considering a point source at $(x_0, y_0, 0)$ and the plane of projection has points $(xcos\theta, xsin\theta, d)$ where θ varying form 0 to 2π and d is the distance between center of the source plane and the target plane.

Now the illuminance expression can be written as

$$E(x,\theta,d) = d^m L_{LED}\left((x_0 - xcos\theta)^2 + (y_0 - xsin\theta)^2 + d^2\right)^{\frac{-(m+2)}{2}} \tag{2.2}$$

where, L_{LED} is the radiance of the LED $(Wm^{-2}Sr^{-1})$

2.2 Arrangement of LED's considered

Following arrangements of LED's are being considered.

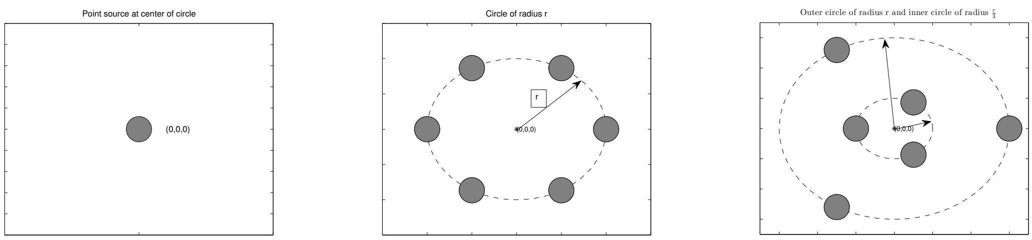

Figure 2.1: System Models considered

- Single LED source is placed at the center of the source circle of radiance L_{LED}
- Six LED sources are placed on the circumference of the circle of radius r with radiance $\frac{L_{LED}}{6}$ uniformly
- Three LED sources are placed on the circumference of the circle of radius r and three on the circumference of the circle of radus $\frac{r}{3}$.

2.2.1 Point source placed at the center of the circle

Considering a point source at the center of the circle $(0,0,0)$ i.e., $x_0 = 0$ and $y_o = 0$. Hence the irradiance expression can be written as,

$$E1(x,\theta,d) = d^m L_{LED}\left(x^2 + d^2\right)^{\frac{-(m+2)}{2}} \tag{2.3}$$

Figure 2.2 represent the irradiance plot on the projection plane with r=5,R=5r,d=10 and m=70.

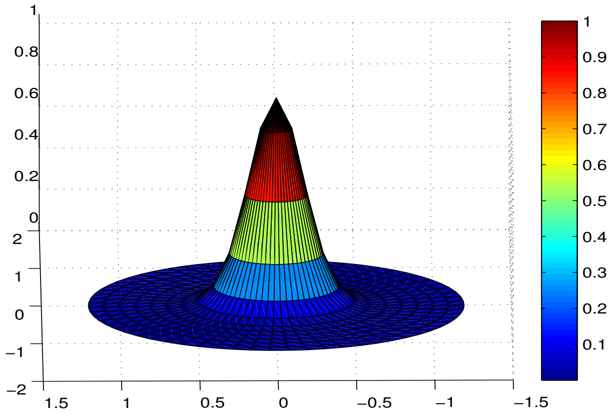

Figure 2.2: LED placed at the center of the circle

Now we can calculate the average value over area for the expression of irradiance. Here $dA = xdxd\theta$ and the expression is averaged over x and θ. x takes values between 0 and R since R is the radius of the plane considered.

$$\begin{aligned}
E1_{avg}(x,\theta,d) &= \frac{d^m L_{LED}}{\pi R^2}\int_0^{2\pi}\int_0^R \frac{xdxd\theta}{(x^2+d^2)^{\frac{m+2}{2}}} \\
&= \frac{d^m L_{LED}}{\pi R^2}(2\pi)\int_0^R \frac{x}{(x^2+d^2)^{\frac{m+2}{2}}}dx \\
&= \frac{d^m L_{LED}}{R^2}\int_0^R \frac{2x}{(x^2+d^2)^{\frac{m+2}{2}}}dx \\
&= \frac{d^m L_{LED}}{R^2}\left(\frac{(x^2+d^2)^{-\frac{m}{2}}}{\frac{-m}{2}}\right)_0^R \\
&= \frac{d^m L_{LED}}{R^2}\frac{2}{m}\left((d^2)^{-m/2}-(d^2+R^2)^{-m/2}\right) \\
&= \frac{2d^m L_{LED}}{mR^2}\left(\frac{1}{d^m}-\frac{1}{(\sqrt{d^2+R^2})^m}\right) \qquad (2.4)
\end{aligned}$$

Peak to Average Value

The maximum value of irradiance of a point source placed at the center ie., equation 2.3 is

$$E1_{peak} = d^m L_{LED}\left(d^2\right)^{\frac{-(m+2)}{2}} \qquad (2.5)$$

The expression for peak to average value is

$$R1_{led} = \frac{d^m L_{LED}\left(d^2\right)^{\frac{-(m+2)}{2}}}{\frac{2d^m L_{LED}}{mR^2}\left(\frac{1}{d^m}-\frac{1}{(\sqrt{d^2+R^2})^m}\right)}$$

$$R1_{led} = \frac{mR^2}{2d^{m+2}} \frac{1}{\left(\frac{1}{d^m} - \frac{1}{(\sqrt{d^2+m^2})^m}\right)}$$
$$= \frac{mR^2}{2d^2} \frac{(\sqrt{d^2+m^2})^m}{(\sqrt{d^2+m^2})^m - d^m}$$
$$= \frac{m}{2}\left(\frac{R}{d}\right)^2 \frac{\left(1+\left(\frac{m}{d}\right)^2\right)^m}{\left(1+\left(\frac{m}{d}\right)^2\right)^m - 1} \tag{2.6}$$

2.2.2 Six LED's placed on the circumference of the circle of radius r uniformly

Let the LED's are placed on the circle at $(rcos\phi, rsin\phi, 0)$ where ϕ takes values from the set $\Phi = \{0, \frac{\pi}{3}, \frac{2\pi}{3}, \pi, \frac{4\pi}{3}, \frac{5\pi}{3}\}$.

Now the expression for the intensity at any point on the circle of radius R.

$$E2(x,\theta,d) = \sum_{\phi \epsilon \Phi} \frac{d^m L_{LED}}{(r^2+x^2+d^2-2xrcos(\theta-\phi))^{\frac{m+2}{2}}} \tag{2.7}$$

Figures. 2.3 and 2.4 represent the individual and sum of individual irradiance plots. LED's average

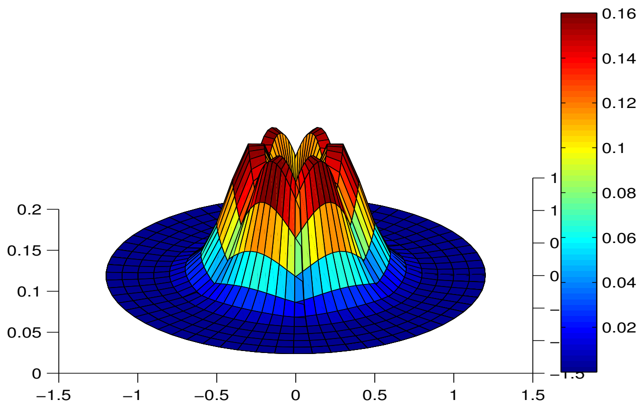

Figure 2.3: Individual plots at six LED's

intensity over any plane parallel to the source surface is always equal for all the LED's present at a constant radius. Hence the average intensity will just be 6 times that of value obtained at $\phi = 0$

$$E2_{avg}(x,\theta,d) = 6\frac{d^m \frac{L_{LED}}{6}}{\pi R^2} \int_0^{2\pi} \int_0^R \frac{xdxd\theta}{(r^2+x^2+d^2-2xrcos(\theta))^{\frac{m+2}{2}}} \tag{2.8}$$

From [27, (3.645)] we have the following integral

$$\frac{1}{2}\int_0^{2\pi} \frac{dx}{(a+bcosx)^{n+1}} = \frac{\pi}{2^n(a+b)^n\sqrt{a^2-b^2}} \sum_{k=0}^{n} \frac{(2n-2k-1)!!(2k-1)!!}{(n-k)!k!} \left(\frac{a+b}{a-b}\right)^k$$

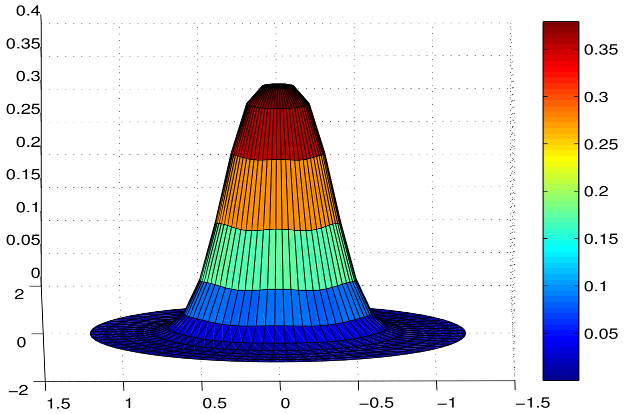

Figure 2.4: Sum of all irradiance plots

Rewriting our integral in terms of above and asuming m to be even we get,

$$E2_{avg}(x,\theta,d) = \frac{d^m L_{LED}}{\pi R^2}\int_0^R x \sum_{k=0}^{(m/2)} \frac{2\pi(m-2k-1)!!(2k-1)!!}{2^{(m/2)}((m/2)-k)!k!}\times \frac{(d^2+r^2+x^2-2xr)^{k-m/2}}{(d^2+r^2+x^2+2kr)^k\sqrt{(d^2+r^2+x^2)^2-(2xr)^2}}dx$$

$$E2_{avg}(x,\theta,d) = \frac{d^m L_{LED}}{2^{(m/2)-1}R^2}\sum_{k=0}^{(m/2)} \frac{(m-2k-1)!!(2k-1)!!}{((m/2)-k)!k!}\times \int_0^R \frac{x(d^2+r^2+x^2-2xr)^{k-m/2}}{(d^2+r^2+x^2+2kr)^k\sqrt{(d^2+r^2+x^2)^2-(2xr)^2}}dx$$

$$E2_{avg}(x,\theta,d) \;=\; \frac{d^m L_{LED}}{2^{(m/2)-1}R^2}\sum_{k=0}^{(m/2)} \frac{(m-2k-1)!!(2k-1)!!}{((m/2)-k)!k!}\int_0^R \frac{x((x-r)^2+d^2)^{k-\frac{m+1}{2}}}{((x+r)^2+d^2)^{k+\frac{1}{2}}}dx \quad (2.9)$$

2.2.3 Three LED's placed on circumference of outer circle and three on the circumference of inner circle of radius $\frac{r}{3}$ uniformly

Let three LED's are placed on the circle at $(rcos\phi, rsin\phi, 0)$ where ϕ_1 takes values from the set $\Phi_1 = \{0, \frac{2\pi}{3}, \frac{4\pi}{3}\}$.

$$E3_1(x,\theta,d) = \sum_{\phi_1 \epsilon \Phi_1} \frac{d^m L_{LED}}{(r^2+x^2+d^2-2xrcos(\theta-\phi_1))^{\frac{m+2}{2}}} \quad (2.10)$$

Other three LED's are placed on the circumference of circle of radius $\frac{r}{3}$ at angles of $\Phi_2 = \{\frac{\pi}{3}, \pi, \frac{5\pi}{3}\}$.

$$E3_2(x,\theta,d) = \sum_{\phi_2 \epsilon \Phi_2} \frac{d^m L_{LED}}{(\left(\frac{r}{3}\right)^2+x^2+d^2-2x\frac{r}{3}cos(\theta-\phi_2))^{\frac{m+2}{2}}} \quad (2.11)$$

Now the expression for the intensity at any point on the circle of radius R

$$E3(x,\theta,d) = \sum_{\phi_1 \epsilon \Phi_1} \frac{d^m L_{LED}}{(r^2+x^2+d^2-2xrcos(\theta-\phi_1))^{\frac{m+2}{2}}} + \sum_{\phi_2 \epsilon \Phi_2} \frac{d^m L_{LED}}{((\frac{r}{3})^2+x^2+d^2-2x\frac{r}{3}cos(\theta-\phi_2))^{\frac{m+2}{2}}} \tag{2.12}$$

Figures. 2.5 and 2.6 represent the individual and sum of irradiance profiles on the projected surface.

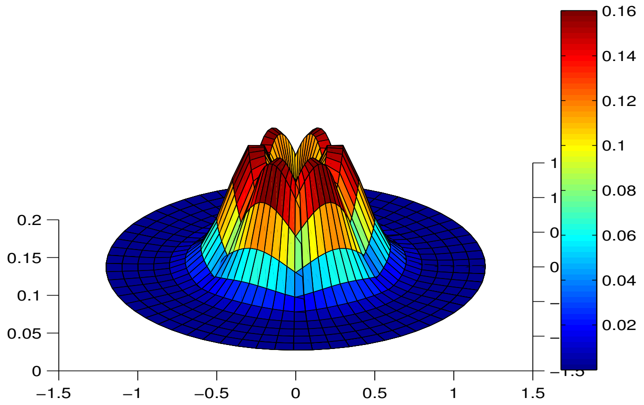

Figure 2.5: Individual intensity plots

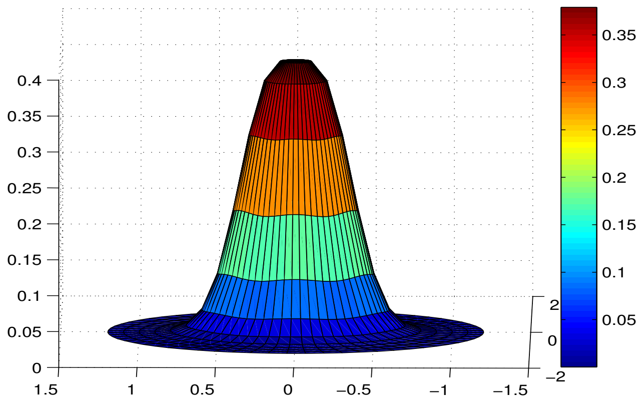

Figure 2.6: Sum of all Intensity plots

LED's average intensity over any plane parallel to the source surface is always equal for all the LED's present at a constant radius.

$$\begin{aligned} E3_{avg}(x,\theta,d) = {} & 3\frac{d^m \frac{L_{LED}}{6}}{\pi R^2}\int_0^{2\pi}\int_0^R \frac{xdxd\theta}{(r^2+x^2+d^2-2xrcos(\theta))^{\frac{m+2}{2}}} \\ & + 3\frac{d^m \frac{L_{LED}}{6}}{\pi R^2}\int_0^{2\pi}\int_0^R \frac{xdxd\theta}{((\frac{r}{3})^2+x^2+d^2-2x\frac{r}{3}cos(\theta))^{\frac{m+2}{2}}} \end{aligned} \tag{2.13}$$

From [27, (3.645)] we have the following integral

$$\frac{1}{2}\int_0^{2\pi}\frac{dx}{(a+bcosx)^{n+1}}=\frac{\pi}{2^n(a+b)^n\sqrt{a^2-b^2}}\sum_{k=0}^{n}\frac{(2n-2k-1)!!(2k-1)!!}{(n-k)!k!}\left(\frac{a+b}{a-b}\right)^k$$

Rewriting our integral in terms of above and asuming m to be even we get,

$$E3_{avg}(x,\theta,d)=\frac{d^mL_{LED}}{2\pi R^2}\int_0^R x\sum_{k=0}^{(m/2)}\frac{2\pi(m-2k-1)!!(2k-1)!!}{2^{(m/2)}((m/2)-k)!k!}\times$$
$$\left(\frac{(d^2+r^2+x^2-2xr)^{k-m/2}}{(d^2+r^2+x^2+2kr)^k\sqrt{(d^2+r^2+x^2)^2-(2xr)^2}}+\frac{(d^2+\left(\frac{r}{3}\right)^2+x^2-2x\frac{r}{3})^{k-m/2}}{(d^2+\left(\frac{r}{3}\right)^2+x^2+2k\frac{r}{3})^k\sqrt{(d^2+\left(\frac{r}{3}\right)^2+x^2)^2-(2x\frac{r}{3})^2}}\right)dx$$

$$E3_{avg}(x,\theta,d)=\frac{d^mL_{LED}}{2^{(m/2)}R^2}\sum_{k=0}^{(m/2)}\frac{(m-2k-1)!!(2k-1)!!}{((m/2)-k)!k!}\times$$
$$\int_0^R\left(\frac{x(d^2+r^2+x^2-2xr)^{k-\frac{m}{2}}}{(d^2+r^2+x^2+2kr)^k\sqrt{(d^2+r^2+x^2)^2-(2xr)^2}}+\frac{x(d^2+\left(\frac{r}{3}\right)^2+x^2-2x\frac{r}{3})^{k-\frac{m}{2}}}{(d^2+\left(\frac{r}{3}\right)^2+x^2+2k\frac{r}{3})^k\sqrt{(d^2+\left(\frac{r}{3}\right)^2+x^2)^2-(2x\frac{r}{3})^2}}\right)dx$$

$$E2_{avg}(x,\theta,d)=\frac{d^mL_{LED}}{2^{(m/2)}R^2}\sum_{k=0}^{(m/2)}\frac{(m-2k-1)!!(2k-1)!!}{((m/2)-k)!k!}\times$$
$$\int_0^R\left(\frac{x((x-r)^2+d^2)^{k-\frac{m+1}{2}}}{((x+r)^2+d^2)^{k+\frac{1}{2}}}+\frac{x((x-\frac{r}{3})^2+d^2)^{k-\frac{m+1}{2}}}{((x+\frac{r}{3})^2+d^2)^{k+\frac{1}{2}}}\right)dx \quad (2.14)$$

2.3 Metric that defines the best case

The following are the metrices considered to define the best case

- Coverage
- Average Irradiance over area

2.4 Results and Discussion

All the plots in this section were drawn with values of r=0.25,R=5r,d=1 and m=30.

Observing the plots in Figure. 2.7 we observe that the coverage is high for case 2 compared to that of case1 ie., the point source. At the center over some radius point source perform better, where as over the remaining annulus case where point sources placed on the circumference perform better.

Similarly observing plots in Figure. 2.8 we observe the coverage in case 3 is higher compared to that of point sources.

Figure. 2.9 contains comparision of case 2 and case 3, wrt to coverage we cannot define anything since case 2 performs over case 3 at some parts and case 3 performs over case 2 in other parts.

Hence Average Irradiance can be calculated for both case 2 and case 3 and the one that have higher average value perform better than the other.

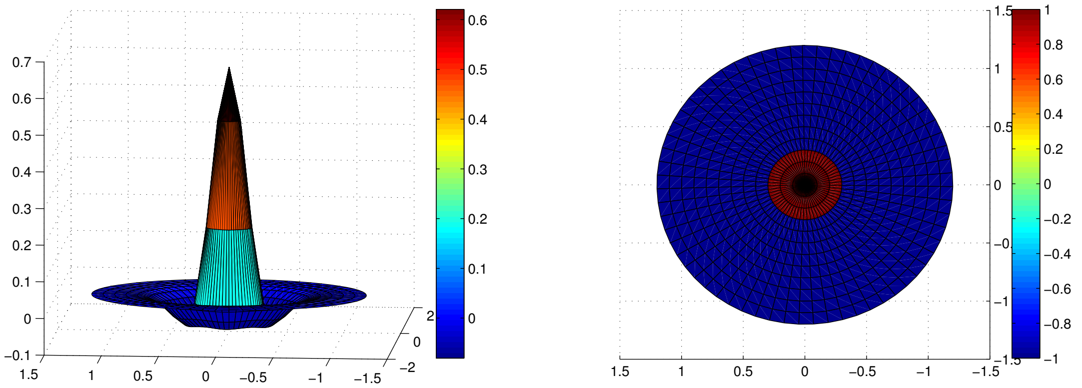

(a) Difference plot

(b) Sign of difference plot

Figure 2.7: Comparing case 1 and case 2

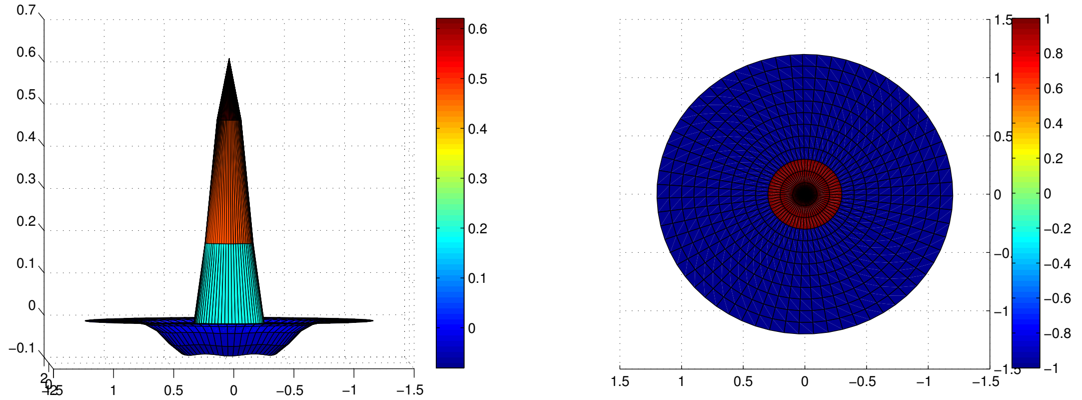

(a) Difference plot

(b) Sign of difference plot

Figure 2.8: Comparing case 1 and case 3

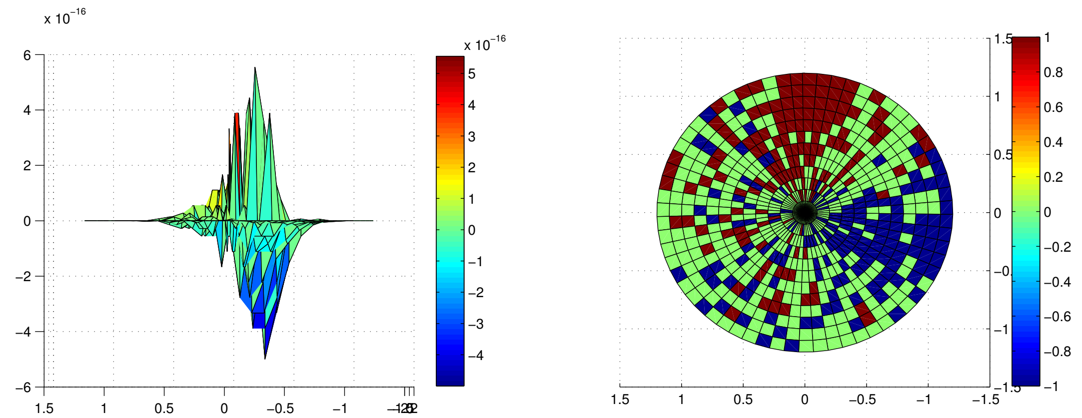

(a) Difference plot

(b) Sign of difference plot

Figure 2.9: Comparing case 2 and case 3

Table. 2.1 contains various values of Average Irradiance for case1,case 2 and case 3 at varying r,R,d,m. And we observe Average Irradiance of case 3 is higher compared to other cases.

r	R	d	m	case1	case 2	case 3
0.25	5r	1	30	0.0427	0.0432	0.0488
0.25	5r	1	20	0.0641	0.0643	0.0696
0.25	5r	1	10	0.1270	0.1265	0.1310
0.25	10r	1	30	0.0107	0.0108	0.0122
0.25	10r	1	50	0.0064	0.0066	0.0080
0.25	3r	1	20	0.1759	0.1721	0.1874

Table 2.1: Average intensities of all the cases over area

Therefore Case 3 ie., case where three LED's placed on the circumference of outer circle and three on the circumference of the inner circle of radius $\frac{r}{3}$ performs over the remaining arrangements.

2.5 Conclusion

Hence placing LEDs on the circumference improves the coverage area of the LEDs when compared to a LED placed at the center of the circle. Where as the irradiance at the center of the region where all the point LEDs are projecting, will be low for the case where LEDs are placed on the circumference compared to a point source at the center.

To improve this we can place three LEDs on the circumference of the circle and three on the circumference of the inner circle uniformly. This improves performance at the center compared to all LEDs placed on the circumference case. It will degrade the performance at the edges compared to case where all LEDs placed on the circumference but not as much as where a LED placed at the center of circle.

Chapter 3

Outage Probability for Directional WLAN for Log-normal Shadowing and Fading

3.1 Introduction

The latest IEEE 802.11ad based wireless local area networks (WLANs) operate on the GHz band[7].At such a high frequency, the received signal power can frequently drop below the required threshold resulting in an outage event. Thus, probability of an outage event, referred to as outage probability, becomes an important system level performance metric. Even for the existing WLAN standards that operate on relatively lower frequencies like IEEE 802.11ac [2], outage probability becomes an important issue for higher pathloss exponents (denoted by α).

In this direction, outage probability has been expressed for a directional carrier sense multiple access/collision avoidance (CSMA/CA) based WLANs in [3]. The analytical expression in [3] is in the form of multiple integrals in the presence of shadowing and Rayleigh fading for pathloss exponent α equal to 4. However, closed form or simplified expressions for the outage probabilities in the presence of shadowing, Nakagami-m fading (of which Rayleigh is a special case), and other pathloss exponents (like $\alpha = 2$) are required. This is the motivation of this work.

The primary contributions of this thesis are as follows. Firstly, the issue of outage probability for the directional WLAN in the presence of Log-normal shadowing, Nakagami-m fading (including the Rayleigh case), and arbitrary pathloss exponent is investigated and suitable expression in terms of integrals is obtained. Secondly, for the typically experienced value of pathloss exponent α equal to 2 a closed form expression in the form of easily computable series summation is derived. Further, for α equal to 4, an approximate closed form expression is obtained. Simulation results are presented that show that the derived results closely match with the expected values.

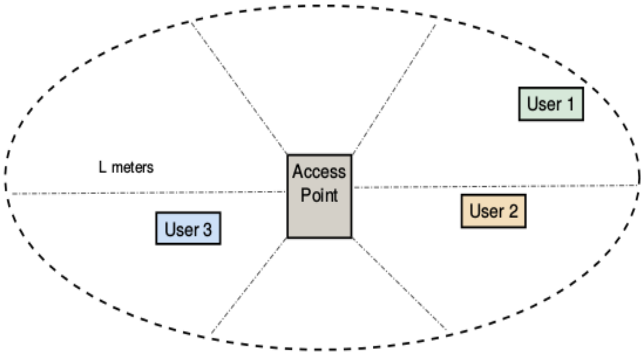

Figure 3.1: System model.

3.2 System Model

We consider a CSMA/CA based WLAN system with an access point (AP) at the center as depicted in Figure. 3.1. The AP has M directional antennas each corresponding to one of the M sectors. The 3-dB beamwidth of any directional antenna is denoted by θ_{3dB}. There exist N users that are contending for access such that the users are uniformly distributed with in a coverage area of radius L.

Let us focus on a random user at a distance r from the AP in a sector such that $r \leq L$. For this user, let θ denote the incident angle and $G(\theta)$ represents the corresponding directivity gain. Then, the probability distribution functions (pdfs) of θ and r are given by [4]

$$f_\Theta(\theta) = \begin{cases} \frac{1}{2\theta_{3dB}} & -\theta_{3dB} < \theta < \theta_{3dB} \\ 0 & \text{otherwise} \end{cases}, \tag{3.1}$$

$$f_R(r) = \begin{cases} \frac{2r}{L^2}, & 0 < r < L \\ 0 & \text{otherwise} \end{cases}. \tag{3.2}$$

Further, the directivity gain is equal to

$$G(\theta) = \frac{\theta_{3dB}}{\pi}. \tag{3.3}$$

Let P_T denote the transmit power of any user. Then, the received signal power at the AP from the user under consideration is equal to

$$P = P_T r^{-\alpha} G(\theta) 10^{\xi/10} x^2, \tag{3.4}$$

where, $\xi \sim \mathcal{N}\left(0, \sigma^2\right)$ represents the Log-normal shadowing coefficient in dB, α is the pathloss exponent considered and x considered is the fading coefficient which can be Rayleigh or Nakagami-m.

Considering z to be Rayleigh fading coefficient,the pdf of z is given by

$$f_Z(z) = \begin{cases} 2ze^{-z^2} & z > 0 \\ 0 & otherwise \end{cases} \tag{3.5}$$

and, considering x to be Nakagami-m fading coefficient. The pdf of x is given by

$$f_X(x) = \begin{cases} \frac{2}{\Gamma(m)} \left(\frac{m}{\Omega}\right)^m x^{2m-1} e^{\frac{-mx^2}{\Omega}} & x > 0 \\ 0 & \text{otherwise} \end{cases} \tag{3.6}$$

where m and Ω are the parameters of the Nakagami-m distribution such that $m > 0.5$ and $\Omega > 0$. Note that $\Gamma(m)$ is the standard Gamma function such that $\Gamma(m) = (m-1)!$ when m is an integer. We consider only integer values of m in this thesis.

Given the received power in (3.4), the SNR of the user under consideration can be defined as

$$SNR = \frac{P}{N_0}\,, \tag{3.7}$$

where, N_0 is the noise power. Thus, the frame outage probability for Rayleigh and Nakagami fadings are defined as follows [3].

3.2.1 For Rayleigh Fading with path loss exponent 4

$$\begin{aligned} P_o &= \Pr\{\text{SNR} < z_0\} \\ &= \Pr\left\{\frac{P}{N_0} < z_0\right\} \qquad (3.8) \\ &= \Pr\left\{\frac{P_T r^{-4} G(\theta) 10^{\xi/10} z^2}{N_0} < z_0\right\}. \\ &= \Pr\left\{z^2 < \frac{z_0 N_0}{P_T r^{-4} G(\theta) 10^{\xi/10}}\right\} \\ &= \Pr\left\{y < \frac{z_0 N_0}{P_T r^{-4} G(\theta) 10^{\xi/10}}\right\} \qquad (3.9) \\ &= F_Y\left(\frac{z_0 N_0}{P_T r^{-4} G(\theta) 10^{\xi/10}}\right), \end{aligned}$$

where $y = z^2$ and z_0 is the SNR threshold. Note that y is obtained from a normalized Rayleigh distribution and will have a cumulative distribution function (CDF) given by [5],

$$F_Y(y) = Pr\{Y \le y\} = 1 - e^{-y} \tag{3.10}$$

By averaging over respective PDF's the average value of outage probability becomes

$$P_o = \int_{-\theta_{3dB}}^{\theta_{3dB}} \int_{-\infty}^{\infty} \int_{0}^{L} F_Y\left(\frac{z_0 N_0}{P_T r^{-4} G(\theta_i) 10^{\xi/10}}\right) f_R(r) f_\Xi(\xi) f_\Theta(\theta)\, dr\, d\xi\, d\theta. \tag{3.11}$$

3.2.2 For Nakagami Fading with α as pathloss exponent

$$\begin{aligned} P_o &= \Pr\{\text{SNR} < z_0\} = \Pr\left\{\frac{P}{N_0} < z_0\right\} \qquad (3.12) \\ &= \Pr\left\{\frac{P_T r^{-\alpha} G(\theta) 10^{\xi/10} x^2}{N_0} < z_0\right\} \\ &= \Pr\left\{x^2 < \frac{z_0 N_0}{P_T r^{-\alpha} G(\theta) 10^{\xi/10}}\right\} \\ &= \Pr\left\{y < \frac{z_0 N_0}{\Omega P_T r^{-\alpha} G(\theta) 10^{\xi/10}}\right\} \qquad (3.13) \\ &= F_Y\left(\frac{z_0 N_0}{\Omega P_T r^{-\alpha} G(\theta) 10^{\xi/10}}\right) \end{aligned}$$

where, $y = x^2/\Omega$ and z_0 denotes the required SNR threshold. Note that y is obtained from a normalized Nakagami-m distribution and will have a cumulative distribution function (CDF) given by [5], for integer m,

$$F_Y(y) = Pr\{Y \leq y\} = 1 - e^{-my} \sum_{i=0}^{m-1} \frac{(m)^i y^i}{(i)!}\,. \qquad (3.14)$$

By averaging over the respective pdfs, the outage probability in (3.12) can be expressed as

$$P_o = \int_{-\theta_{3dB}}^{\theta_{3dB}} \int_{-\infty}^{\infty} \int_{0}^{L} F_Y\left(\frac{z_0 N_0}{\Omega P_T r^{-2} G(\theta) 10^{\xi/10}}\right) f_R(r) f_\Xi(\xi) f_\Theta(\theta) dr d\xi d\theta\,. \qquad (3.15)$$

Substituting the expressions from (3.1), (3.2), (3.3), and (3.14) in (3.15) and integrating with respect to θ results in

$$P_o = \int_{-\infty}^{\infty} \int_{0}^{L} \left[1 - \sum_{i=0}^{m-1} e^{-m\left(\frac{\pi z_0 N_0}{\theta_{3dB} \Omega P_T r^{-\alpha} 10^{\xi/10}}\right)} \frac{\left(\frac{\pi m z_0 N_0}{\theta_{3dB} \Omega P_T r^{-\alpha} 10^{\xi/10}}\right)^i}{i!}\right] \frac{2r}{L^2} \frac{e^{\frac{-\xi^2}{2\sigma^2}}}{\sqrt{2\pi}\sigma} dr d\xi \qquad (3.16)$$

Given this system setting, the outage probability for a single user for α equal to 2 and 4 is derived next.

3.3 Outage Probability Derivation

3.3.1 Outage Probability for Rayleigh Fading with $\alpha = 4$

Substituting (3.1) and (3.3) in (3.11), and integrating w.r.t. θ results in

$$P_o = \int_{-\infty}^{\infty} \int_{0}^{L} F_Y\left(\frac{z_0 N_0 \pi}{P_T r^{-4} \theta_{3dB} 10^{\xi/10}}\right) f_R(r) f_\Xi(\xi) dr d\xi\,. \qquad (3.17)$$

Using (3.2) and expanding $f_{\Xi}(\xi)$, the expression in (3.17) becomes

$$\begin{aligned} P_o &= \int_{-\infty}^{\infty} \int_{0}^{L} \left(1 - e^{-z_0 \frac{N_0}{P_T} \frac{\theta_{3dB}}{\pi} r^4 10^{-\xi/10}}\right) e^{\frac{-\xi^2}{2\sigma^2}} \frac{2r}{L^2} \frac{1}{\sqrt{2\pi}\sigma} dr d\xi \\ &= 1 - \int_{-\infty}^{\infty} \int_{0}^{L^2} \left(e^{-z_0 \frac{N_0}{P_T} \frac{\theta_{3dB}}{\pi} 10^{-\xi/10} t^2}\right) e^{\frac{-\xi^2}{2\sigma^2}} \frac{1}{\sqrt{2\pi}\sigma} dt d\xi, \\ &= 1 - \int_{-\infty}^{\infty} \frac{e^{\frac{-\xi^2}{2\sigma^2}}}{\sqrt{2\pi}\sigma L^2} \int_{0}^{L^2} e^{-a(\xi)t^2} dt d\xi \,, \end{aligned} \tag{3.18}$$

where,

$$a(\xi) = z_0 \frac{N_0}{P_T} \frac{\theta_{3dB}}{\pi} 10^{-\xi/10} \,. \tag{3.19}$$

The expression in (3.18) can be evaluated in the form of Q-function as follows.

$$P_o = 1 - \frac{1}{\sqrt{2\pi}\sigma L^2} \int_{-\infty}^{\infty} \frac{\sqrt{\pi}}{2\sqrt{a(\xi)}} e^{\frac{\xi^2}{2\sigma^2}} \left(1 - 2Q(\sqrt{2a(\xi)}L^2)\right) d\xi \,. \tag{3.20}$$

Substituting $a(\xi)$ in (3.20) results in

$$P_o \;=\; 1 \;-\; \frac{1}{2\sqrt{2}\sigma L^2} \sqrt{\frac{\pi P_T}{2z_0 N_0 \theta_{3dB}}} \int_{-\infty}^{\infty} e^{\frac{-\xi^2}{2\sigma^2}} 10^{\xi/20} \left(1 - 2Q\sqrt{\frac{2z_0 N_0 \theta_{3dB} L^4}{P_T \pi}} 10^{\xi/20}\right) d\xi \,. \tag{3.21}$$

Let,

$$b_1 = \frac{1}{2\sigma L^2} \sqrt{\frac{\pi P_T}{z_0 N_0 \theta_{3dB}}} \text{ and } b_2 = \sqrt{\frac{2z_0 N_0 \theta_{3dB} L^4}{P_T \pi}} \,. \tag{3.22}$$

Then, (3.21) can be expressed as

$$\begin{aligned} P_o &= 1 - b_1 \int_{-\infty}^{\infty} e^{\frac{-\xi^2}{2\sigma^2}} 10^{\xi/20} \left[1 - 2Q\left(b_2 10^{-\xi/20}\right)\right] d\xi \\ &= 1 - b_1 \int_{-\infty}^{\infty} e^{\frac{-\xi^2}{2\sigma^2}} 10^{\xi/20} d\xi \quad + 2b_1 \int_{-\infty}^{\infty} e^{\frac{-\xi^2}{2\sigma^2}} 10^{\xi/20} 2Q\left(b_2 10^{-\xi/20}\right) d\xi \,. \end{aligned} \tag{3.23}$$

Note that for the range of values of interest, the second integral in (3.23) can be neglected and we obtain

$$\begin{aligned} P_o &\approx 1 - b_1 \int_{-\infty}^{\infty} e^{\frac{-\xi^2}{2\sigma^2}} 10^{\xi/20} d\xi \\ &= 1 - b_1 \sqrt{2\pi}\sigma e^{(\sigma \ln(10))^2/800} \,. \end{aligned} \tag{3.24}$$

The expression in (3.24) *is one of the main results of this thesis* and can be easily computed for various values of all the parameters involved. Next, we derive the results for Nakagami fading with $\alpha = 2$.

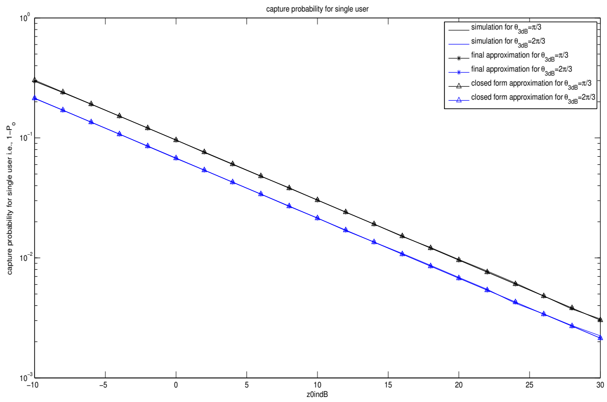

Figure 3.2: Variation of (1-P_0), where P_0 is the outage probability of Rayleigh Fading versus the SNR threshold z_0.

3.3.2 Outage Probability for Nakagami Fading with $\alpha = 2$

In (3.16), substituting $\alpha = 2$ and $r^2 = t$ results in

$$P_o = 1 - \int_{-\infty}^{\infty}\int_{0}^{L^2}\left(\sum_{i=0}^{m-1} e^{-m\left(\frac{\pi z_0 N_0 t}{\theta_{3dB}\Omega P_T 10^{\xi/10}}\right)} \frac{\left(\frac{\pi z_0 N_0 m t}{\theta_{3dB}\Omega P_T 10^{\xi/10}}\right)^i}{i!}\right)\frac{1}{L^2}\frac{e^{\frac{-\xi^2}{2\sigma^2}}}{\sqrt{2\pi}\sigma}dtd\xi \tag{3.25}$$

Let,

$$\beta(\xi) = \frac{\pi m z_0 N_0 10^{-\xi/10}}{\theta_{3dB}\Omega P_T}\,. \tag{3.26}$$

Then (3.25) can be written as

$$P_o = 1 - \int_{-\infty}^{\infty}\int_{0}^{L^2}\sum_{i=0}^{m-1} e^{-\beta(\xi)t}\frac{(\beta(\xi)t)^i}{i!}\frac{e^{\frac{-\xi^2}{2\sigma^2}}}{L^2\sqrt{2\pi}\sigma}dtd\xi\,, \tag{3.27}$$

which can be further expressed as

$$P_o = 1 - \sum_{i=0}^{m-1}\int_{-\infty}^{\infty}\frac{e^{\frac{-\xi^2}{2\sigma^2}}}{L^2\sqrt{2\pi}\sigma}\frac{(\beta(\xi))^i}{i!}\int_{0}^{L^2} t^i e^{-\beta(\xi)t}dtd\xi\,. \tag{3.28}$$

After appropriate substitution,

$$\begin{aligned} P_o &= 1 - \sum_{i=0}^{m-1}\int_{-\infty}^{\infty}\frac{e^{\frac{-\xi^2}{2\sigma^2}}}{L^2\sqrt{2\pi}\sigma i!\beta(\xi)}\int_{0}^{\beta(\xi)L^2} e^{-r}r^i drd\xi \qquad (3.29)\\ &= 1 - \sum_{i=0}^{m-1}\int_{-\infty}^{\infty}\frac{e^{\frac{-\xi^2}{2\sigma^2}}}{L^2\sqrt{2\pi}\sigma\beta(\xi)}\left(1 - \sum_{k=0}^{i}\frac{(\beta(\xi)L^2)^k e^{-\beta(\xi)L^2}}{k!}\right)d\xi\,. \end{aligned}$$

using [27, (3.351.1)]. Rearranging the terms in (3.29) results in

$$P_o \quad = \quad 1 - \underbrace{\int_{-\infty}^{\infty} \frac{m e^{\frac{-\xi^2}{2\sigma^2}}}{\sqrt{2\pi}\sigma L^2 \beta(\xi)} d\xi}_{I_1} + \underbrace{\sum_{i=0}^{m-1} \int_{-\infty}^{\infty} \frac{e^{\frac{-\xi^2}{2\sigma^2}}}{L^2\sqrt{2\pi}\sigma\beta(\xi)} \left(\sum_{k=0}^{i} \frac{(\beta(\xi)L^2)^k e^{-\beta(\xi)L^2}}{k!} \right) d\xi}_{I_2} \,. \tag{3.30}$$

From [27, (3.321.3)],

$$I_1 = \int_{-\infty}^{\infty} \frac{m e^{\frac{-\xi^2}{2\sigma^2}}}{\sqrt{2\pi}\sigma L^2 \beta(\xi)} d\xi = \frac{\theta_{3dB}\Omega P_T}{\pi z_0 N_0 L^2} e^{\frac{(\sigma log(10))^2}{200}} \,. \tag{3.31}$$

after substituting for $\beta(\xi)$ from (3.26). Similarly,

$$\begin{aligned} I_2 &= \sum_{i=0}^{m-1} \int_{-\infty}^{\infty} \frac{e^{\frac{-\xi^2}{2\sigma^2}}}{L^2\sqrt{2\pi}\sigma\beta(\xi)} \left(\sum_{k=0}^{i} \frac{(\beta(\xi)L^2)^k e^{-\beta(\xi)L^2}}{k!} \right) d\xi \\ &= \sum_{i=0}^{m-1} \sum_{k=0}^{i} \int_{-\infty}^{\infty} \frac{e^{\frac{-\xi^2}{2\sigma^2}}}{\sqrt{2\pi}\sigma} \frac{(\frac{\pi m z_0 N_0 10^{-\xi/10}}{\theta_{3dB}P_t} L^2)^{k-1} e^{-\frac{\pi m z_0 N_0 10^{-\xi/10}}{\theta_{3dB}\Omega P_T} L^2}}{k!} d\xi \,. \end{aligned} \tag{3.32}$$

Let,

$$B = \frac{\pi m z_0 N_0 L^2}{\theta_{3dB}\Omega P_T} \,. \tag{3.33}$$

Then,

$$I_2 = \sum_{i=1}^{m} \sum_{k=0}^{i} \frac{B^{k-1}}{k!\sqrt{2\pi}\sigma} \int_{-\infty}^{\infty} e^{\frac{-\xi^2}{2\sigma^2}} 10^{\frac{-\xi(k-1)}{10}} e^{-B10^{-\xi/10}} d\xi \,. \tag{3.34}$$

Using the power series expansion for the exponential in the above integral we obtain,

$$\begin{aligned} \int_{-\infty}^{\infty} e^{\frac{-\xi^2}{2\sigma^2}} 10^{\frac{-\xi(k-1)}{10}} e^{-B10^{-\xi/10}} d\xi &= \sum_{j=0}^{N} \frac{(-B)^j}{j!} \int_{-\infty}^{\infty} e^{\frac{-\xi^2}{2\sigma^2}} 10^{\frac{-\xi(k-1+j)}{10}} d\xi \\ &= \sum_{j=0}^{N} \frac{(-B)^j}{j!} e^{\frac{((k+j-1)\sigma log(10))^2}{200}} \,. \end{aligned} \tag{3.35}$$

Thus,

$$I_2 = \sum_{i=0}^{m-1} \sum_{k=0}^{i} \frac{B^{k-1}}{k!\sqrt{2\pi}\sigma} \sum_{j=0}^{N} \frac{(-B)^j}{j!} e^{\frac{((k+j-1)\sigma log(10))^2}{200}} \,. \tag{3.36}$$

Substituting the expressions from (3.31) and (3.36) in (3.30), we obtain

$$P_o = 1 - \frac{\theta_{3dB}\Omega P_T}{\pi z_0 N_0 L^2} e^{\frac{(\sigma log(10))^2}{200}} + \sum_{i=0}^{m-1} \sum_{j=0}^{N} \sum_{k=0}^{i} \frac{(-1)^j B^{k+j-1}}{j!k!\sqrt{2\pi}\sigma} e^{\frac{((k+j-1)\sigma log(10))^2}{200}} \,. \tag{3.37}$$

The expression in (3.37) *is second main results of this thesis* and can be easily computed for various values of all the parameters involved. Next, we derive the results for $\alpha = 4$.

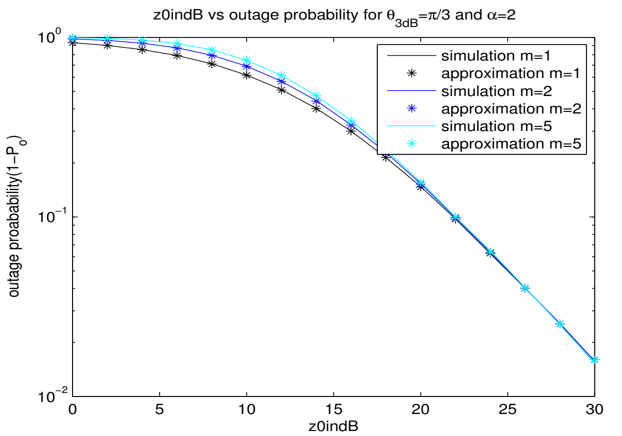

Figure 3.3: Variation of one minus the outage probability (1-P_o) with the SNR threshold (z_0), for a path loss exponent of 2 and $\theta_{3dB} = \pi/3$.

3.3.3 Outage Probability for Nakagami Fading with $\alpha = 4$

For pathloss exponent $\alpha = 4$, the outage probability in (3.12) can be expressed using the approach in the previous subsection as

$$P_o = 1 - \int_{-\infty}^{\infty} \int_{0}^{L} \sum_{i=0}^{m-1} e^{-\beta(\xi)r^4} \frac{(\beta(\xi)r^4)^i}{i!} \frac{(2r)e^{\frac{-\xi^2}{2\sigma^2}}}{L^2\sqrt{2\pi}\sigma} dr d\xi \,, \tag{3.38}$$

which after appropriate substitution results in,

$$P_o = 1 - \sum_{i=0}^{m-1} \int_{-\infty}^{\infty} \frac{(\beta(\xi))^{-0.5}}{2(i)!} \frac{e^{\frac{-\xi^2}{2\sigma^2}}}{\sqrt{2\pi}\sigma L^2} \int_{0}^{\beta(\xi)L^4} e^{-t} t^{i-\frac{1}{2}} dt d\xi \,. \tag{3.39}$$

The expression in (3.39) can be simplified to

$$P_o = 1 - \sum_{i=0}^{m-1} \int_{-\infty}^{\infty} \frac{(\beta(\xi))^{-0.5}}{2(i)!} \frac{e^{\frac{-\xi^2}{2\sigma^2}}}{\sqrt{2\pi}\sigma L^2} \gamma\left(i + \frac{1}{2}, \beta(\xi)L^4\right) d\xi \,, \tag{3.40}$$

where, $\gamma(\cdot,\cdot)$ is the incomplete gamma function [26, (6.5.2)]. From [26, (6.5.3)],

$$\gamma(x,a) = \Gamma(a) - \Gamma(x,a) \,,$$

which implies the following inequality

$$\gamma(x,a) < \Gamma(a) \,. \tag{3.41}$$

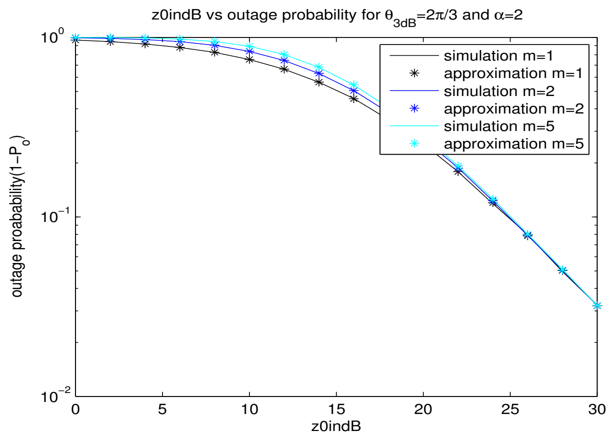

Figure 3.4: Variation of one minus the outage probability (1-P_o) with the SNR threshold (z_0), for a path loss exponent of 2 and $\theta_{3dB} = 2\pi/3$.

From (3.40) and (3.41), we can obtain a bound on P_o. Thus,

$$P_o \leq 1 - \sum_{i=0}^{m-1} \int_{-\infty}^{\infty} \frac{(\beta(\xi))^{-0.5}}{2(i)!} \frac{e^{\frac{-\xi^2}{2\sigma^2}}}{\sqrt{2\pi}\sigma L^2} \Gamma\left(i + \frac{1}{2}\right) d\xi \,. \tag{3.42}$$

Substituting the value of $\beta(\xi)$ from (3.26) in the previous expression,

$$\begin{aligned} P_0 &\leq 1 - \sum_{i=0}^{m-1} \int_{-\infty}^{\infty} \frac{e^{\frac{-\xi^2}{2\sigma^2}} \left(\frac{\theta_{3dB}\Omega P_T}{\pi m Z_0 N_0 10^{-\xi/10}}\right)^{\frac{1}{2}}}{\sqrt{2\pi}\sigma L^2 2(i)!} \Gamma\left(i + \frac{1}{2}\right) d\xi \\ &= 1 - \sum_{i=0}^{m-1} \frac{\Gamma\left(i + \frac{1}{2}\right) \left(\frac{\theta_{3dB}\Omega P_T}{\pi m Z_0 N_0}\right)^{\frac{1}{2}}}{\sqrt{2\pi}\sigma L^2 2(i)!} \int_{-\infty}^{\infty} e^{\frac{-\xi^2}{2\sigma^2}} 10^{\xi/20} d\xi \,. \end{aligned} \tag{3.43}$$

The integral in (3.43) can be solved using [27, (3.321.3)] resulting in

$$P_o = 1 - \sum_{i=0}^{m-1} \frac{\Gamma\left(i + \frac{1}{2}\right) \left(\frac{\theta_{3dB}\Omega P_T}{\pi m Z_0 N_0}\right)^{\frac{1}{2}}}{L^2 2(i)!} e^{\frac{(\sigma log(10))^2}{800}} \,. \tag{3.44}$$

The expression in (3.44) *is the third main result of this thesis..* Next, we present the numerical results, comparing the derived results with those obtained from simulation.

3.4 Numerical Results

In this section, we compare the analytical expressions derived in the previous section with results obtained through Monte-Carlo simulations. For simulations, we consider an AP at the center with a circular coverage area of radius $L = 100$ m. The users are uniformly randomly distributed in this region. We consider $\sigma = 6$ dB, $P_T = 20$ dBm, and $N_0 = -90$ dBm as in [3]. For a single user in the system, the variation of one minus the outage probability of Rayleigh Fading versus z_0 is plotted in

Figure. 3.2 . As observed from Figure. 3.2, the closed form approximation in (3.24) matches closely with the results generated through simulations for various values beam widths (θ_{3dB}= 60 and 120 degrees).

The value of Nakagami distribution parameter m is taken as $m \in \{1, 2, 5\}$ and $\Omega = 1$. For a single user in the system, the variation of one minus the outage probability (1-P_o) versus the SNR threshold (z_0) is plotted in Figure. 3.3 and Figure. 3.4 for a pathloss exponent of $\alpha = 2$ and the beam widths (θ_{3dB}) equal to $\pi/3$ and $2\pi/3$ degrees, respectively. The closed form approximation results for various m are obtained by substituting suitable values in (3.37). It is observed from Figure. 3.3 and Figure. 3.4, that the closed form approximation derived in (3.37) matches closely with the results generated through simulations for various values of beam widths.

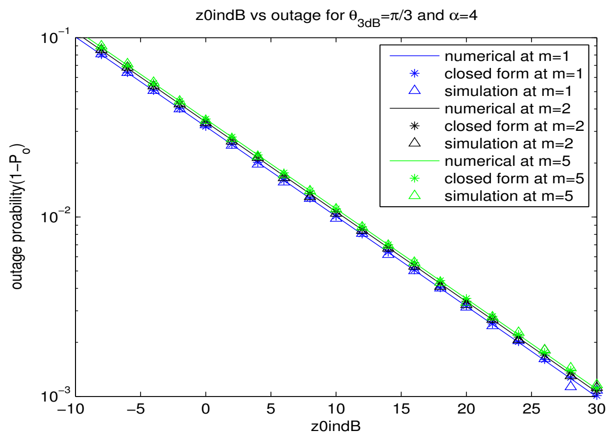

Figure 3.5: Variation of one minus the outage probability (1-P_o) with the SNR threshold (z_0), for a path loss exponent of 4 and $\theta_{3dB} = \pi/3$.

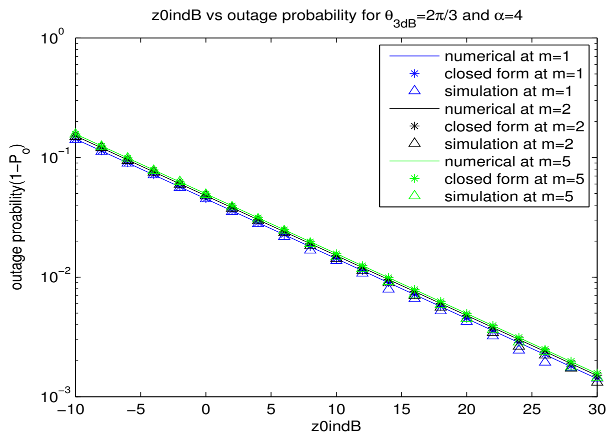

Figure 3.6: Variation of one minus the outage probability (1-P_o) with the SNR threshold (z_0), for a path loss exponent of 4 and $\theta_{3dB} = 2\pi/3$.

In Figure. 3.5 and Figure. 3.6, the variation of one minus the outage probability (1-P_o) versus the SNR threshold (z_0) is presented for a pathloss exponent of $\alpha = 4$ and the beam widths (θ_{3dB})

equal to $\pi/3$ and $2\pi/3$ degrees, respectively. It can be observed that the closed form approximation for a path loss exponent of $\alpha = 4$ given in (3.44) is a good approximation of the results obtained through simulations for varying values of z_0.

3.5 Conclusions

We have considered a directional WLAN system in the presence of Log-normal shadowing and Rayleigh and Nakagami-m fading considering. We have derived approximate expression for outage probability for single user for two different pathloss exponents (α equal to 2 and 4) in Nakagami fading case and for $\alpha = 4$ in Rayleigh fading case. Further, we have compared the derived results with simulation results and shown that they match closely. In future, similar expressions of outage probabilities for a more diverse physical setting can be derived.

References

[1] IEEE, "Wireless LAN Medium Access Control (MAC) and Physical Layer (PHY) Specifications Amendment 3: Enhancements for Very High Throughput in the 60 GHz Band," *IEEE Standards Association Standard 802.11ad*, 2012.

[2] IEEE, "Wireless LAN Medium Access Control (MAC) and Physical Layer (PHY) Specifications–Amendment 4: Enhancements for Very High Throughput for Operation in Bands below 6 GHz," *IEEE Standards Association Standard 802.11ac*, 2013.

[3] L. Wang, et al., "A Cross-Layer investigation for the throughput performance of CSMA/CA-based WLANs with directional antennas and capture effect," IEEE Trans. Veh. Technol., vol. 56, no. 5, pp. 2756–2766, Sep. 2007.

[4] C. T. Lau and C. Leung, "Capture models for mobile packet radio networks," IEEE Trans. Commun., vol. 40, no. 5, pp. 917–925, May 1992.

[5] J. Proakis and M. Salehi, "Digital Communications," 5th Edition, *McGraw-Hill*, Boston, 2007.

[6] I. S. Gradshteyn and I. M. Rhyzik, "Table of Integrals, Series and Products," *Elsevier/Academic Press*, Sixth edition, 1964.

[7] J. H. Kim and J. K. Lee, "Capture effects of wireless CSMA/CA protocols in Rayleigh and shadow fading channel ," IEEE Trans. Veh. Technol., vol. 48, no. 4, pp. 1277–1286, Jul. 1999.

[8] M. Abramowitz and I. A. Stegun, "Abramowitz and Stegun: Handbook of Mathematical Functions," *Dover Publications*, First edition, 1964.

[9] M. Benitez and F. Casadevall, "Versatile, accurate, and analytically tractable approximation for the Gaussian Q-function," *IEEE Trans. Comm.* vol. 59, no. 4, pp. 917–922, Feb. 2011.

[10] Qian Chen, et al., "Directional Cooperative MAC Protocol Design and Performance Analysis for IEEE 802.11ad WLANs," IEEE Trans. Veh. Technol., vol. 62, no. 6, pp. 2667–2677, July 2013.

[11] E. F. Schubert, J. K. Kim, Solid-state light sources getting smart, Science 308, 12741278 (2005)

[12] Y. Narukawa, White-light LEDs, Opt. Photonics News 15, 2429 (2004).

[13] J. Kovc, J. Jakabovic, and M. Kytka, Advanced light emitting devices for optoelectronic applications, Proc. SPIE 7138, 71382A (2008).

[14] I. Moreno, Configuration of LED arrays for uniform illumination, Proc. SPIE 5622, 713718 (2004).

[15] S. K. Kopparapu, Lighting design for machine vision application, Image Vis. Comput. 24(7), 720726 (2006).

[16] I. Moreno, Design of LED spherical lamps for uniform far-field illumination, Proc. SPIE 6046, 60462E (2006).

[17] N. Wittels, and M. A. Gennert, Optimal lighting design to maximize illumination uniformity, SPIE 2348, 46 56 (1994).

[18] H. Yang, J. W. M. Bergmans, T. C. W. Schenk, J.-P. M. G. Linnartz, and R. Rietman, Uniform illumination rendering using an array of LEDs: a signal processing perspective, IEEE Trans. Signal Process. 57(3), 1044 1057 (2009).

[19] M. A. Gennert, N. Wittels, and G. L. Leatherman, Uniform frontal illumination of planer surfaces: where to place the lamps, Opt. Eng. 32(6), 12611271 (1993).

[20] I. Moreno, M. Avendao-Alejo, and R. I. Tzonchev, Designing light- emitting diode arrays for uniform near field irradiance, Appl. Op- tics 45, 22652272 (2006).

[21] Z. Qin, K. Wang, F. Chen, X. B. Luo, and S. Liu, Analysis of condition for uniform lighting generated by array of light emit- ting diodes with large view angle, Opt. Express 18, 1746017476 (2010).

[22] A. J. W. Whang, Y. Y. Chen, and Y. T. Teng, Designing uniform illumination systems by surface-tailored lens and configurations of LED arrays, J. Disp. Technol. 5(3), 94103 (2009).

[23] J. Tan, K. Yang, M. Xia, and Y. Yang, Analysis of uniform illu- mination system with imperfect Lambertian LEDs, Opt. Appl. 41, 507517 (2011).

[24] K. Wang, D. Wu, Z. Qin, F. Chen, X. B. Luo, and S. Liu, New revers- ing design method for LED uniform illumination, Opt. Express 19, 830840 (2011).

[25] H. Yang, J. W. M. Bergmans, T. C. W. Schenk, J. P. M. G. Linnartz, and R. Rietman, Uniform illumination rendering using an array of LEDs: a signal processing perspective, IEEE T. Signal Proces. 57, 10441057 (2009).

[26] M. Abramowitz and I. A. Stegun, “Abramowitz and Stegun: Handbook of Mathematical Functions,” *Dover Publications*, First edition, 1964.

[27] I. S. Gradshteyn and I. M. Rhyzik, “Table of Integrals, Series and Products,” *Elsevier/Academic Press*, Sixth edition, 1964.

[28] Sridhara, “FREE SPACE OPTICAL COMMUNICATION ,” *International Journal of Latest Research in Science and Technology., vol. 1, Issue. 3, pp. 202-205, September-October (2012)*

[29] Hu Guo-yong , Chen Chang-ying , Chen Zhen-qiang , “Free-Space Optical communication using visible light ,” *Journal of Zhejiang University SCIENCE A., vol. 8, Issue. 2, pp. 186-191,Feb-2007*

[30] Petr Lobaz and Petr Vanek, "Safe range of free space light propagation calculation in single precision ," *Optics Express., vol. 23, Issue. 3, pp. 3260-3269,2015*

[31] The Physics Hyper Textbook,
`http://physics.info/intensity`

[32] `https://en.wikipedia.org/wiki/Interference_(wave_propagation)`